

# Mapping Glutamatergic Drive in the Vertebrate Retina With a Channel-Permeant Organic Cation

ROBERT E. MARC\*

John Moran Eye Center, University of Utah School of Medicine, Salt Lake City, Utah 84132

## ABSTRACT

Patterns of neuronal excitation in complex populations can be mapped anatomically by activating ionotropic glutamate receptors in the presence of 1-amino-4-guanidobutane (AGB), a channel-permeant guanidinium analogue. Intracellular AGB signals were trapped with conventional glutaraldehyde fixation and were detected by probing registered serial thin sections with anti-AGB and anti-amino acid immunoglobulins, revealing both the accumulated AGB and the characteristic neurochemical signatures of individual cells. In isolated rabbit retina, both glutamate and the ionotropic glutamate receptor agonists  $\alpha$ -amino-3-hydroxyl-5-methylisoxazole-4-propionic acid (AMPA), kainic acid (KA), and N-methyl-D-aspartic acid (NMDA) activated permeation of AGB into retinal neurons in dose-dependent and pharmacologically specific modes. Horizontal cells and bipolar cells were dominated by AMPA/KA receptor activation with little or no evidence of NMDA receptor involvement. Strong NMDA activation of AGB permeation was restricted to subsets of the amacrine and ganglion cell populations. Threshold agonist doses for the most responsive cell groups (AMPA, 300 nM; KA, 2  $\mu$ M; NMDA, 63  $\mu$ M; glutamate, 1 mM) were similar to values obtained from electrophysiological and neurotransmitter release measures. The threshold for activation of AGB permeation by exogenous glutamate was shifted to <200  $\mu$ M in the presence of the glutamate transporter antagonist dihydrokainate, indicating substantial spatial buffering of extracellular glutamate levels in vitro. Agonist-activated permeation of AGB into neurons persisted under blockades of Na<sup>+</sup>-dependent transporters, voltage-activated Ca<sup>+</sup> and Na<sup>+</sup> channels, and ionotropic  $\gamma$ -aminobutyric acid and glycine receptors. Cholinergic agonists evoked no permeation. *J. Comp. Neurol.* 407:47-64, 1999. © 1999 Wiley-Liss, Inc.

**Indexing terms:** glutamate receptors; immunocytochemistry; 1-amino-4-guanidobutane

Glutamic acid mediates fast synaptic output from vertebrate retinal photoreceptor and bipolar cells largely through ionotropic receptors on second- and third-order neurons (Hensley et al., 1993; Slaughter and Miller, 1983a,b), with the exception of the transduction of photoreceptor  $\rightarrow$  ON-center bipolar cell signals by a metabotropic glutamate receptor (Slaughter and Miller, 1981; Nakajima et al., 1993). Because 50-100 unique cell types arrayed in planar densities of from 50 to >8,000/mm<sup>2</sup> comprise the neural retina (Vaney, 1990; Kolb et al., 1981; Wässle et al., 1994), and because expressions of  $\alpha$ -amino-3-hydroxyl-5-methylisoxazole-4-propionic acid (AMPA), kainic acid (KA), or N-methyl-D-aspartate (NMDA) receptor subclasses in varied densities and combinations may occur for each type, maps of ionotropic glutamatergic drive that resolve defined populations cannot be derived easily from unit recording, calcium (Ca<sup>2+</sup>) imaging, receptor immunocytochemistry, or in situ hybridization techniques. Immunocytochemical data suggest that mammalian horizontal cells

express glutamate receptor (GluR) KA receptor subunits GluR6/7 (Morigawa et al., 1995; Peng et al., 1995; Brandstätter et al., 1996), but other data imply that horizontal cells also express AMPA receptors (Qin and Pourcho, 1996). In addition to subunit combinations, mixtures of entire AMPA/KA receptors may differentially mediate glutamate responses of many mammalian retinal neurons (Massey and Miller, 1987, 1990; Linn et al., 1991; Cohen et al., 1994; Zhou et al., 1994; Cohen and Miller, 1995; Zhou and Fain, 1995; Sasaki and Kaneko, 1996).

NMDA receptors seem to be restricted largely to ganglion cells and to subsets of amacrine cells (Massey and

Grant sponsor: National Institutes of Health; Grant number: EY02576.

\*Correspondence to: Robert E. Marc, John Moran Eye Center, University of Utah School of Medicine, 75 N. Medical Drive, Salt Lake City, UT 84132. E-mail: robert.marc@hsc.utah.edu

Received 20 February 1998; Revised 11 November 1998; Accepted 1 December 1998

Miller, 1990; Linn and Massey, 1991; Cohen and Miller, 1994) and are likely to coexist with AMPA/KA receptors at postsynaptic sites (Diamond and Copenhagen, 1993; Velte et al., 1997). Glutamate receptor subtype composition can impact absolute and incremental ligand responsivities, temporal band pass (Lomeli et al., 1994; Mosbacher et al., 1994; Partin et al., 1996; Sekiguchi et al., 1997), ionic selectivities of postsynaptic currents (Gieger et al., 1995; Washburn et al., 1997), and perhaps determine additional gating conditions. In turn, receptor composition and number across cell types will impact "visual" properties, such as absolute and incremental photic thresholds, dynamic ranges, temporal tuning, and perhaps some forms of adaptation. Even so, the distribution of a single ionotropic AMPA receptor subunit typically admits no physiologic interpretation without knowing key members of the entire receptor subunit assembly in a single cell type (see, e.g., Washburn et al., 1997). Physiologic studies in retina have rarely been able to characterize agonist sensitivities across cell types, more often defining cells as generic groups, such as "ganglion cells." Thus, we have been seeking methods that preserve some degree of structural information and cellular identity to augment receptor immunocytochemistry, mRNA expression patterns, and physiologic characterizations.

Quantitative patterns of excitation can be tracked across large groups of identifiable cell types with channel-permeant organic cation probes. Guanidinium cation analogues permeate a range of "nonselective" cation channels, including nicotinic acetylcholine-gated channels in muscle (Dwyer et al., 1980; Dwyer, 1986; Hille, 1992) and neuronal cells (Yoshikami, 1981; Qwik, 1985; Loring, 1990), serotonin-3 (5HT<sub>3</sub>)-gated channels in neurons (Emerit et al., 1993), cyclic nucleotide-gated channels in sensory cells (Nakatani and Yau, 1988; Picco and Menini 1993; Balasubramanian et al., 1995; Kramer and Tibbs, 1996), ATP-gated P<sub>2X</sub> receptor channels (Evans et al., 1996), and neuronal Na<sup>+</sup> channels (see, e.g., Rang and Ritchie, 1988; Reith, 1990). The guanidinium analogue 1-amino-4-guanidobutane (AGB; Fig. 1), commonly known as "agmatine," has a planar guanidinium head and seems to be capable of entering the outer vestibule of nonselective cation channels, fully traversing some channels. The influx of radiolabeled AGB has been used as a measure of ligand-gated channel permeation (see, e.g., Yoshikami, 1981; Qwik, 1985; Kuzirian et al., 1986), and this paper now demonstrates that integrated fluxes of unlabeled AGB activated by ligands selective for AMPA/KA and NMDA receptors can be measured in identified retinal cell types with AGB-selective immunoglobulins (IgGs). The conditions for visualizing the ligand-gated AGB signal are consistent with AGB permeation through ionotropic glutamate receptor-channel complexes and the pharmacology and dose-dependencies of agonist activations measured by AGB permeations in retina match those reported by using electrophysiological measures.

## MATERIALS AND METHODS

### Isolated retinal preparations

Light-adapted adult male and female albino and pigmented rabbits were tranquilized with intramuscular ketamine/xylazine, deeply anesthetized with intraperitoneal urethane in saline, and killed by thoracotomy, all in accordance with institutional animal care and use guide-

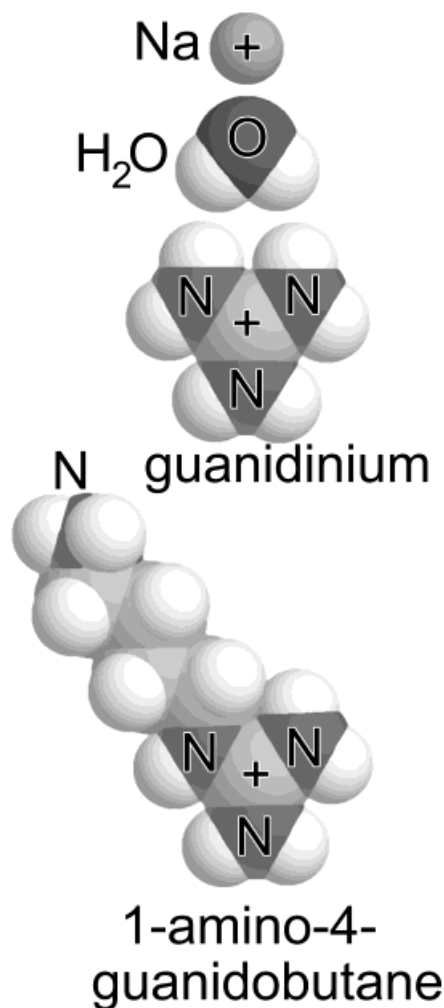


Fig. 1. The structure of 1-amino-4-guanidobutane (AGB; agmatine) compared with a guanidinium cation, water, and a sodium ion scaled to a Pauling sodium crystal radius of 0.95 Å. All molecules were rendered with Roger Sayle's RasMol (<http://klaatu.oit.umass.edu:80/microbio/rasmol/>). Molecular coordinates for both AGB and the guanidinium cation were generated from SMILES strings submitted to the CORINA coordinate engine (<http://schiele.organik.uni-erlangen.de/corina/corina.html>).

lines. Both eyes were removed rapidly and hemisected, and large retinal pieces were mounted on 5- $\mu$ m pore size cellulose acetate filter discs (Whatman, Clifton, NJ), as described for mammalian retinas by Marc and Liu (1985). Retinas were submerged until use, usually within 15 minutes, in 35°C Ames medium (Ames and Nesbett, 1981) equilibrated with 95% O<sub>2</sub>/5% CO<sub>2</sub>. Sets of retinal chips roughly 2 mm  $\times$  3 mm were razor cut from the large pieces and incubated as matched series for 10 minutes at 35°C under gas in 100- $\mu$ l droplets of Ames medium containing 5 mM AGB plus additional reagents (see below). All incubations were performed under fluorescent room lighting with a flux density of  $\approx 2.9 \times 10^4$  photons/second/ $\mu$ m<sup>2</sup> integrated over 400–700 nm at the level of the incubation chamber and peak fluxes of  $3.6 \times 10^3$ ,  $2.7 \times 10^3$ , and  $2.2 \times 10^3$  photons/second/ $\mu$ m<sup>2</sup> at the principal 435-nm, 546-nm, and 572-nm lines. Over 450 individual samples from 35 rabbits were processed. Each retina produced sufficient samples

for two or three complete concentration series with various ligands, and, although they were derived from different retinal regions, otherwise, the samples were handled identically. Some retinas were incubated in D-aspartate (five series; 100  $\mu$ M to 5 mM) to assess glial fractional volumes (see Marc et al., 1995). Reactions were quenched by immersing each chip in room temperature 1% paraformaldehyde, 2.5% glutaraldehyde, 3% sucrose, 0.01%  $\text{CaCl}_2$ , in 0.1 M phosphate buffer, pH 7.4. All tissue was processed as described previously (Marc et al., 1990).

### Specimen preparation and immunocytochemical visualization

Each chip was embedded as a flatmount in epoxy resin on a glass slide, and a portion was scribed from the slide as a small rectangular fragment (Stell and Lightfoot, 1975). Multiple chips from a given chemical series (e.g., a single dose-response set) were assembled into a stack (Marc et al., 1990) and sectioned serially at 250 nm onto 12-spot Teflon-coated slides (Cel-Line; Erie Scientific, Portsmouth, NH). The immunocytochemical and IgG production procedures were as described previously (Marc et al., 1990, 1995) by using the silver-intensification protocol of Kalloniatis and Fletcher (1993). The bovine serum albumin-AGB immunogen was produced by standard hapten coupling methods (Matute and Streit, 1986; Marc et al., 1995) and elicited production of rabbit IgGs selective for protein glutaraldehyde-linked AGB, as determined by dot immunoassays (Marc et al., 1990). Primary IgG signals were detected with goat-anti-rabbit IgGs adsorbed to 1 nm gold particles (Amersham International, Buckinghamshire, United Kingdom) and visualized with silver intensification. Anti-glutamate and anti- $\gamma$ -aminobutyric acid (GABA) IgGs were obtained from Signature Immunologics Inc. (Salt Lake City, UT; the author is a principal of Signature Immunologics). Anti-D-aspartate IgGs were produced in the Marc laboratory at the University of Utah. Single-letter amino acid codes were sometimes used to denote GABA ( $\gamma$ ) and glutamate (E).

### Image analysis

All images of immunoreactivity were captured as eight-bit 512 pixel  $\times$  480 line or 1,197  $\times$  960 frames under constant flux, 550-nm (10 nm band pass) light with a fixed CCD camera gain and gamma with gray value (GV) scales linearly with log concentration over a 2 log unit range. Silver visualization produces density-scaled images, and linear image inversion produces intensity-scaled images. Serial images of GABA, AGB, and glutamate signals were aligned to better than 250 nm root mean square error with registration algorithms from PCI Remote Sensing, Inc. (Richmond Hill, Ontario, Canada). Image analysis, inversion, thresholding, profiling, and response fraction calculations were performed with Image-Pro Plus 2.0 (Media Cybernetics Inc., Silver Spring, MD).

### Response analysis

Three response types were used to assess the behaviors of neuronal populations after glutamate agonist activation.

**Laminar profiles.** Responses at each level of the inner plexiform layer were measured as the mean GV of a horizontal 1  $\times$  100–400 pixel wide strip for every level of the inner plexiform layer at a resolution of 250 nm/pixel. This method reports the agonist levels at which cells that

comprise a given level of the inner plexiform layer are activated and reach saturation. This technique does not require individual cell identification.

**Fractional responses.** The fractional response of the inner plexiform layer to graded agonist doses was defined as the area of the inner plexiform layer reaching a GV of  $\geq 127$ . Because different cell types comprise different volume fractions of the inner plexiform layer and may have different ligand affinities, the fractional response gives a global view of neuronal responsiveness. It reflects the proportion of elements responding to a given ligand at saturation and, again, does not require identification of individual cell types. This method is limited in part by the fact that some ligands, notably glutamate, activate a lower rate of peak permeation regardless of dose. Glutamate fractional response curves were acquired with a criterion GV of 87, corresponding to a 0.3 log unit or twofold increase in detectivity, with some increase in variance.

**Dose-response functions.** True response functions to graded doses of ligand were obtained by sampling directly from known cell populations, such as horizontal cell somata or starburst amacrine cell strata in the inner plexiform layer. It is important to consider the effect of cell volume on each of these measures, although the arguments are not fully derived here. The AGB signal in a neuron depends on cell volume, AGB activity, the number of open channels, and single open-channel AGB permeability. For normalized dose-response functions of a single cell type, the only determinants of the response are number of open channels and single open-channel AGB permeability. Differences in apparent affinities are independent of the cell volume. Differences in cell volume will distort the shapes of the fractional response curves and laminar profiles, but the recruitment fraction obtained at saturation and the spatial distributions of responsive elements are not affected by volume differences.

### Agents and sources

Ames medium was either purchased from Sigma-Aldrich Corp. (St. Louis, MO) or made according to Ames and Nesbett (1981) and modified as needed to produce high  $\text{K}^+$ ,  $\text{Li}^+$ , or AGB salines by equimolar  $\text{Na}^+$  replacement or nominally  $\text{Ca}^{2+}$ -free or  $\text{Mg}^{2+}$ -free salines by exclusion of  $\text{Ca}^{2+}$  or  $\text{Mg}^{2+}$ . No divalent cation buffer systems were used. AGB, D-aspartate, and all other agents at final concentrations of 5 mM or less were added without  $\text{Na}^+$  adjustment. All solutions were made fresh before each rabbit preparation. AGB (agmatine sulfate), isobutylmethylxanthine (IBMX), D-aspartate, L-glutamate, dihydrokainate (DHK), and strychnine hydrochloride were obtained from Sigma-Aldrich Corp. KA, NMDA, AMPA, 1,2,3,4-tetrahydro-6-nitro-2,3-dioxobenzof[quinoxaline-7-sulfonamide (NBQX), cyclodextrin caged 6-cyano-7-nitroquinoxaline-2,3-dione (CNQX), D-2-amino-7-phosphonoheptanoate (D-AP7), epibatidine, picrotoxin, and nimodipine were obtained from Research Biochemicals International (Natick, MA). NBQX and nimodipine were prepared as fresh concentrated stocks in 100% methanol and added to the medium immediately prior to use. Equivalent levels of methanol added to the Ames medium had no impact on ligand-induced permeation. All other agents were made as concentrated stocks in deionized water and were added to the AGB Ames medium just before each experimental series. Conotoxins were a gift from Dr. M. McIntosh of the University of Utah.

### Parametric optimization

Various AGB concentrations (0.1–120 mM; three series) and incubation times (1–60 minutes; two series) were tested to optimize detection of AGB permeation induced by exogenous ligands. High concentrations of AGB yielded strong signals, and the maximal signal at 10 minutes of incubation in 30  $\mu$ M KA was achieved at about 30 mM AGB. Stable signals with little basal labeling were obtained at 5 mM. At longer incubation times (e.g., 20 minutes), even 1 mM AGB led to good signals in the presence of 30  $\mu$ M KA. Extremely high levels of AGB (>20 mM) induced some cell swelling and lysis as well as exposing significant basal signals. KA-activated signals were detectable in 5 mM AGB medium within 120 seconds of exposure, so there is latitude in incubation time. Beyond 15 minutes, substantial basal signaling in the absence of any exogenous ligand begins to appear and is strong by 60 minutes. Basal signaling is largely abolished by 5  $\mu$ M NBQX, which indicates that the AGB method has potential for mapping endogenous excitation events.

### Figure preparation

All images are digital and were assembled from the raw data captured by a CCD camera (see Image analysis, above). Selected frames of raw Tagged Image Format files were extracted for display, each frame was sharpened by unsharp masking, and, after entire images were assembled as a single figure, contrasts were adjusted with linear remapping to correct for out-of-gamut effects during printing. All final images were prepared in Adobe PhotoShop (version 4.0; Adobe Systems, Mountain View, CA).

## RESULTS

### There is no measurable endogenous AGB signal in retina

AGB occurs in diverse organisms as the decarboxylation product of arginine (Hamana et al., 1991; Raasch et al., 1995) and has been proposed as an endogenous ligand for imidazole receptors (Li et al., 1994; however, see also Piletz et al., 1995; Sun et al., 1995; Berdeu et al., 1996). Although AGB levels are low in the brain, and although AGB seems to be restricted to astrocytes in culture (Regunathan et al., 1995), it does appear at significant levels in nonneural tissues (Morrissey et al., 1995). Normal rabbit retina probed with anti-AGB IgGs displays no significant endogenous AGB signal that would confound its use as an excitation probe.

### Basal permeation of AGB occurs at a low rate in acute exposures

Incubation of isolated rabbit retinas for 10 minutes in Ames medium containing 5 mM AGB normally led to no significant neuronal labeling (Fig. 2A) and to variable but weak basal labeling in cone photoreceptors and in a few bipolar cells. AGB appears to induce no acute cytopathology and has no impact on normal amino acid signals in vitro as, demonstrated by  $\gamma \cdot \text{AGB} \cdot \text{E} \rightarrow \text{red-green-blue}$  (rgb) mapping (Fig. 2B;  $\text{GABA} \rightarrow \text{red}$ ,  $\text{AGB} \rightarrow \text{green}$ ,  $\text{glutamate} \rightarrow \text{blue}$ ). The patterns of GABA and glutamate signals are indistinguishable from normal rabbit retina. The AGB signal strength in cones varied across preparations, and no ligand control was achieved. The cone AGB signal was not attenuated by glutamate receptor antago-

nists,  $\text{Ca}^{2+}$  channel blockers, or replacement of  $\text{Na}^{+}$  with  $\text{Li}^{+}$ . It also was not enhanced detectably by  $\text{K}^{+}$  depolarization or phosphodiesterase inhibitors, such as 1 mM IBMX. No AGB entry was observed in rods.

### Ionotropic glutamate receptor agonists activate AGB permeation

Activation of AMPA/KA and NMDA receptors stimulated AGB entry in to retinal neurons (Figs. 2, 3). Inclusion of 100  $\mu$ M AMPA in the medium activated strong AGB signals in many cell types, including horizontal cells, some types of bipolar cells, and many amacrine and ganglion cells (Fig. 2C,D). Horizontal cells display strong AGB signals that generate a characteristic cyan hue in rgb mapped images (Fig. 2D;  $\text{AGB} + \text{E} = \text{green} + \text{blue} = \text{cyan}$ ). The fact that AMPA activates only a small subset of bipolar cells is demonstrated by the absence of AGB signals in a large population of glutamate-rich bipolar cells revealed as blue cells in Figure 2D. Amacrine and ganglion cells varied substantially in their responses to AMPA/KA receptor activations, and this is addressed in the accompanying paper (Marc, 1999). Saturating NMDA doses induced a very different pattern of AGB permeation (Fig. 2E,F). Horizontal cells and bipolar cells were not activated at all, consistent with most physiological reports, but ganglion cells and some amacrine cells responded vigorously. KA activation was very effective and evoked AGB entry into horizontal cells, bipolar cells, amacrine cells, and ganglion cells (Fig. 3). The degree of bipolar, amacrine, and ganglion cell activation clearly exceeded that triggered by AMPA. Analyses of these differences are beyond the scope of this paper but may reflect the fact that KA does not desensitize AMPA receptors, although different AMPA receptor types display varying speeds and degrees of desensitization upon activation by AMPA or glutamate (Lerma et al., 1993; Paternain et al., 1995). Differential activation of different neuronal populations by a single application of agonist can be documented by correlating AGB, glutamate, and GABA signals of individual cells in registered serial 250-nm sections (Fig. 3). For example, in the ganglion cell layer, GABA-positive starburst amacrine cells (see Marc, 1999) and large glutamate-positive ganglion cells show strong AGB signals in response to 100  $\mu$ M KA, whereas certain medium-sized ganglion cells and glutamate-positive/GABA-positive ganglion cells demonstrate little or no induced response. These patterns of labeling derive from distinctive cell populations and do not represent response variations within a class, as shown in the accompanying paper (Marc, 1999). Neither AMPA, KA, nor NMDA induced AGB permeation into photoreceptor or Müller cells.

The natural ligand at all of these synapses is thought to be glutamate. Glutamate proved to be a weak activator of AGB permeation until very high doses (1–5 mM) were used, and, even at saturation, the magnitude of the response was very small, although many cells were recruited to respond (Fig. 4A). The responsive cells were clearly horizontal cells, a subset of bipolar cells, many amacrine cells, and ganglion cells. Unlike the unique patterns of AGB lamination evoked by KA, AMPA, and NMDA, no distinct lamination could be observed in the inner plexiform layer at any level of glutamate activation. This is consistent with the notion that both NMDA and non-NMDA ionotropic systems were activated by glutamate. The maximal signal evoked in any cell by glutamate was very weak—less than one-third of that evoked by

NMDA and KA. Part of the ineffectiveness of glutamate clearly is due to spatial buffering of exogenous glutamate levels by Müller cells. For example, normally, 625  $\mu\text{M}$  glutamate is subthreshold for activating AGB permeation (Fig. 4B) but evoked saturating responses in the presence of 1 mM DHK (Fig. 4C), a level capable of blocking virtually all neuronal and glial glutamate transport in the rabbit retina (Marc, unpublished data). The visual pattern of glutamate-evoked responses resembled summed AMPA and NMDA responses but never reached the overall levels evoked by nondesensitizing KA activation or NMDA. There were some elements that did appear as dark as those in NMDA preparations when glutamate plus DHK was employed, consistent with the fact that NMDA receptors do not desensitize substantially to sustained glutamate levels. However, glutamate-activated horizontal cells, bipolar cells, and many amacrine cells possessed weaker signals than those displayed in KA or AMPA preparations.

### AGB entry is not mediated by Na-coupled transporters or voltage-activated $\text{Ca}^{2+}$ channels

Ligand-activated AGB labeling matches the pattern expected if AGB enters by permeation of ionotropic glutamate receptor-channel complexes, but it is prudent to explore other possible modes of entry, such as uptake or permeation of voltage-gated channels. The involvement of transport was explored by activating AGB signals with glutamate agonists under conditions that were expected to attenuate Na-coupled transport. The outcomes of these experiments led to no alterations in signal patterns, and the images are not reproduced here. Substitution of 120 mM  $\text{Li}^+$  for  $\text{Na}^+$  (four series of four samples each) led to no change in basal or AMPA-, KA-, or NMDA-activated labeling in any cell type. Furthermore, the magnitude of AMPA-, KA-, and NMDA-activated labeling increased with graded replacements of 5 mM, 10 mM, 15 mM, 30 mM, 60 mM, and 120 mM of total  $\text{Na}^+$  with AGB (three series), saturating at about 30 mM AGB, whereas the cell types that were labeled remained unchanged. No experiment supported involvement of Na<sup>+</sup>-coupled transport processes in the labeling patterns reported here.

Voltage-dependent  $\text{Ca}^{2+}$  channels play no discernible role in AGB permeation, because incubation in the presence of the L-type  $\text{Ca}^{2+}$  channel blocker nimodipine (1  $\mu\text{M}$ , 10  $\mu\text{M}$ , and 100  $\mu\text{M}$ ; two series); 0.1–10  $\mu\text{M}$  of conotoxins GVIA, MVIIC, MVIID, and SVIB (two series each); and 100  $\mu\text{M}$   $\text{Cd}^{3+}$  (one series) had no measurable effect on either basal or ligand-induced labeling. This does not mean that AGB cannot permeate  $\text{Ca}^{2+}$  channels but, rather, that the ligand-gated signal cannot be due to a secondarily activated  $\text{Ca}^{2+}$  channel permeation. Another possible mode of entry is through classical voltage-sensitive  $\text{Na}^+$  channels, although such channels seem to be restricted largely to the inner retina. The presence of 1  $\mu\text{M}$  tetrodotoxin (one series of three experiments) had no detectable effect on KA- or NMDA-activated AGB labeling.

Incubations in the presence of graded  $\text{K}^+$ -rich media (6 mM, 12 mM, 25 mM, and 50 mM  $\text{K}^+$  as equimolar replacement of Na; two series) did evoke a weak increase in AGB signal in horizontal cells and diffuse signals in the inner plexiform layer at the highest  $\text{K}^+$  levels but only  $\approx 10\%$  of that induced by saturating doses of KA. This does not necessarily mean that AGB entry involved permeation of voltage-sensitive channels; it is just as likely that

passive depolarization of photoreceptors and bipolar cells induced sufficient glutamate release to be detected by AGB permeation. However, longer integration times are required to obtain robust signals from such endogenous agonist release. However, even at 50 mM  $\text{K}^+$ , neither rod photoreceptors, nor Müller cells, nor most amacrine, bipolar, or ganglion cells showed any significant AGB signals, and, by extension, AGB entry likely is not mediated by a voltage-sensitive mechanism. Furthermore, the weak increase in AGB signals evoked by  $\text{K}^+$  was unaffected by any  $\text{Ca}^{2+}$  channel blockers. Although this was not an exhaustive survey, the hypothesis that any ligand-activated AGB labeling was mediated by either transporters or voltage-gated channels was not supported by any experiment. This is actually a very important outcome, because it shows that agonist-activated acute endogenous glutamate release from bipolar cells cannot evoke a secondary AGB signal in amacrine or ganglion cells that detectably corrupts AMPA-, KA-, or NMDA-activated patterns.

### Quantitative measures of ligand-activated AGB signals

Postembedding immunocytochemistry affords the opportunity to simultaneously compare responses of populations of cells with glutamate agonists. In addition to observing qualitatively different patterns of responsive cells across the retina and varying laminar patterns in the inner plexiform layer, it is possible to quantify population responses as laminar profiles and fractional response functions. The behaviors of individual cell types can be characterized by dose-response functions.

**Laminar profiles of responses in the inner plexiform layer.** Individual  $2 \times 3$  mm pieces from a single retina were incubated in parallel, and each was exposed to a separate ligand dose in a series (20 KA series of 4–6 concentrations; 8 AMPA series of 4–6 concentrations; 12 NMDA series of 4–7 concentrations), then glutaraldehyde quenched, and each series was mounted as a single resin stack (Marc et al., 1990) cut as serial 250-nm sections. Thus, every section contained all dose-response samples for a single series probed under identical conditions. Responses were captured under constant calibrated conditions, and each image was inverted to intensity-scaled form. Figure 5 depicts four examples from a typical KA

Fig. 2. (overleaf)  $\alpha$ -Amino-3-hydroxyl-5-methylisoxazole-4-propionic acid (AMPA)-activated 1-amino-4-guanidobutane (AGB) signals and concurrent  $\gamma$ -aminobutyric acid (GABA), AGB, and glutamate signals viewed as  $\gamma \cdot \text{AGB} \cdot \text{E} \rightarrow \text{red-green-blue}$  (rgb) mappings in rabbit retina after incubation in Ames medium plus 5 mM AGB in the presence and absence of glutamate receptor agonists. **A:** Control AGB signal. Note the absence of significant basal labeling. **B:** Control  $\gamma \cdot \text{AGB} \cdot \text{E} \rightarrow \text{rgb}$  mapping: In the presence of 5 mM AGB, both GABA and glutamate signals are indistinguishable from normal retina. **C:** AGB signal (100  $\mu\text{M}$  AMPA): Horizontal cell ( $\text{h}^+$ ), bipolar cell ( $\text{b}^+$ ), amacrine cell ( $\text{a}^+$ ), and inner plexiform layer (ipl) signals are activated. **D:**  $\gamma \cdot \text{AGB} \cdot \text{E} \rightarrow \text{rgb}$  mapping (100  $\mu\text{M}$  AMPA): Despite activation of some cells, certain bipolar ( $\text{b}^-$ ) and amacrine cells ( $\text{a}^-$ ) are either weakly or completely unresponsive to AMPA. **E:** N-methyl-D-aspartic acid (NMDA; 1,000  $\mu\text{M}$ ). A saturating dose of NMDA activates many elements in the amacrine cell and ganglion cell layers. **F:**  $\gamma \cdot \text{AGB} \cdot \text{E} \rightarrow \text{rgb}$  mapping (1,000  $\mu\text{M}$  NMDA): Horizontal and bipolar cells are unresponsive to NMDA. a, Amacrine cells; b, bipolar cells; gcl, ganglion cell layer; h, horizontal cells; inl, inner nuclear layer; ipl, inner plexiform layer; m, Müller cells; mf, Müller cell foot pieces; onl, outer nuclear layer; opl, outer plexiform layer. g, ganglion cell. Scale bars = 50  $\mu\text{m}$ .

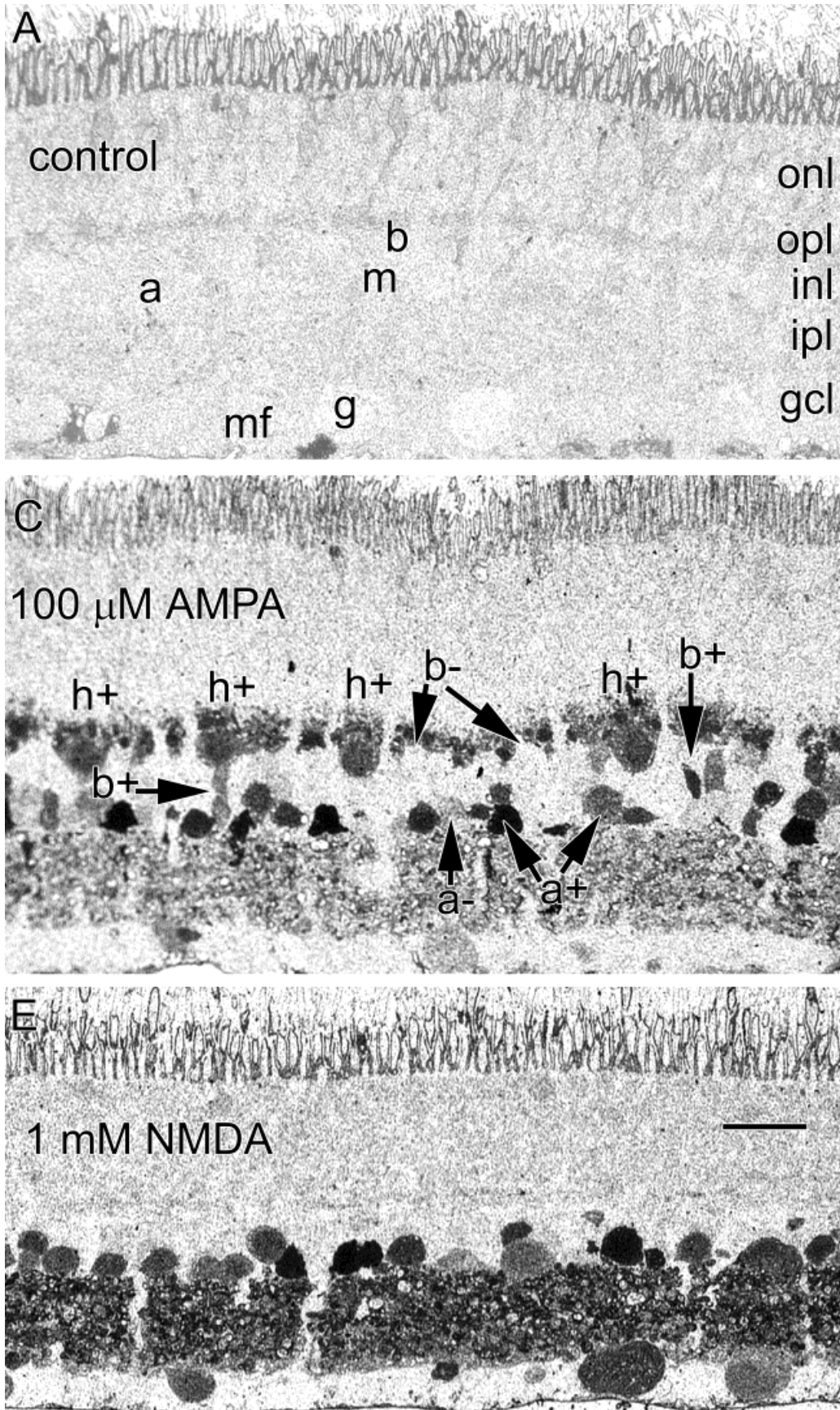


Figure 2

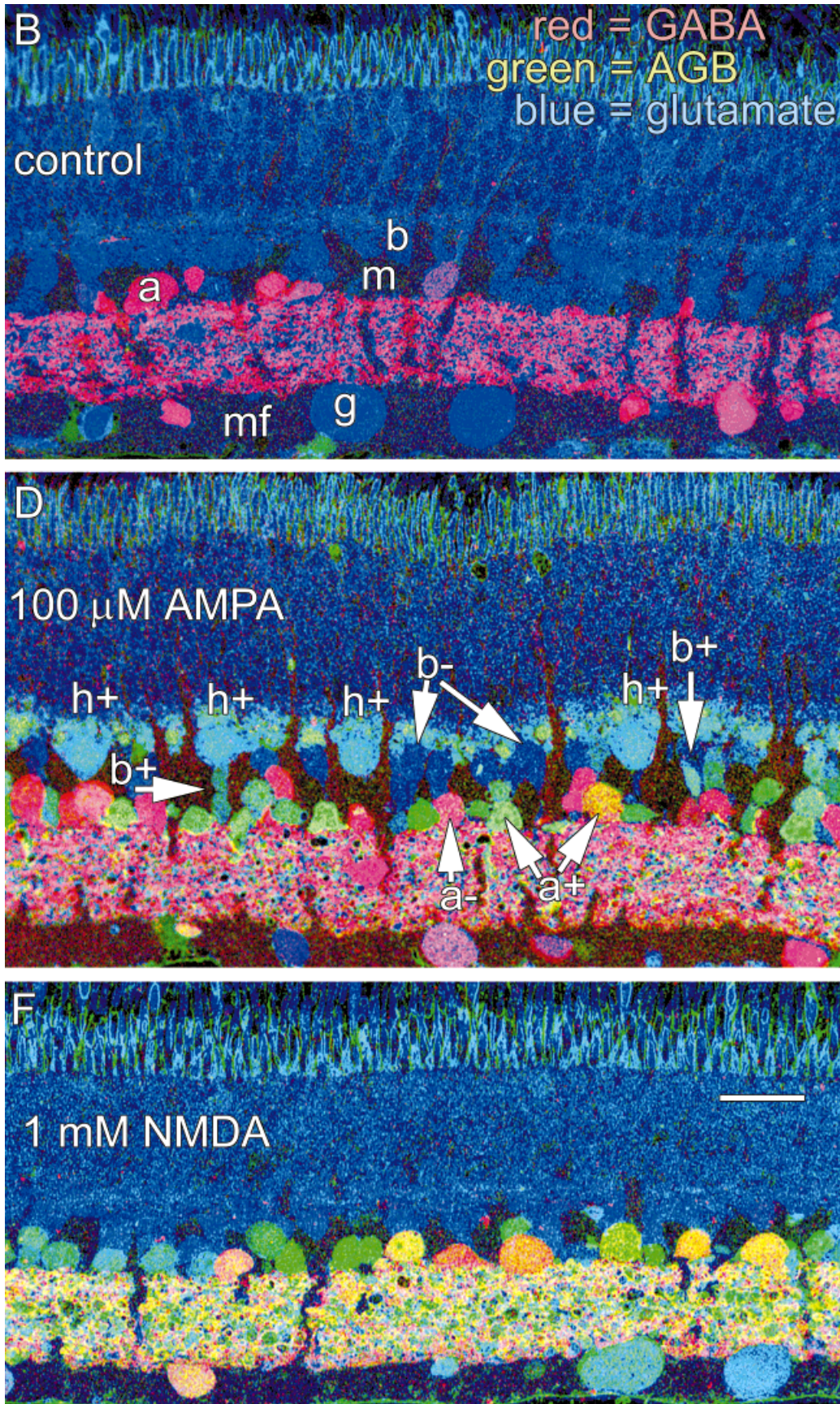


Figure 2 (Continued)

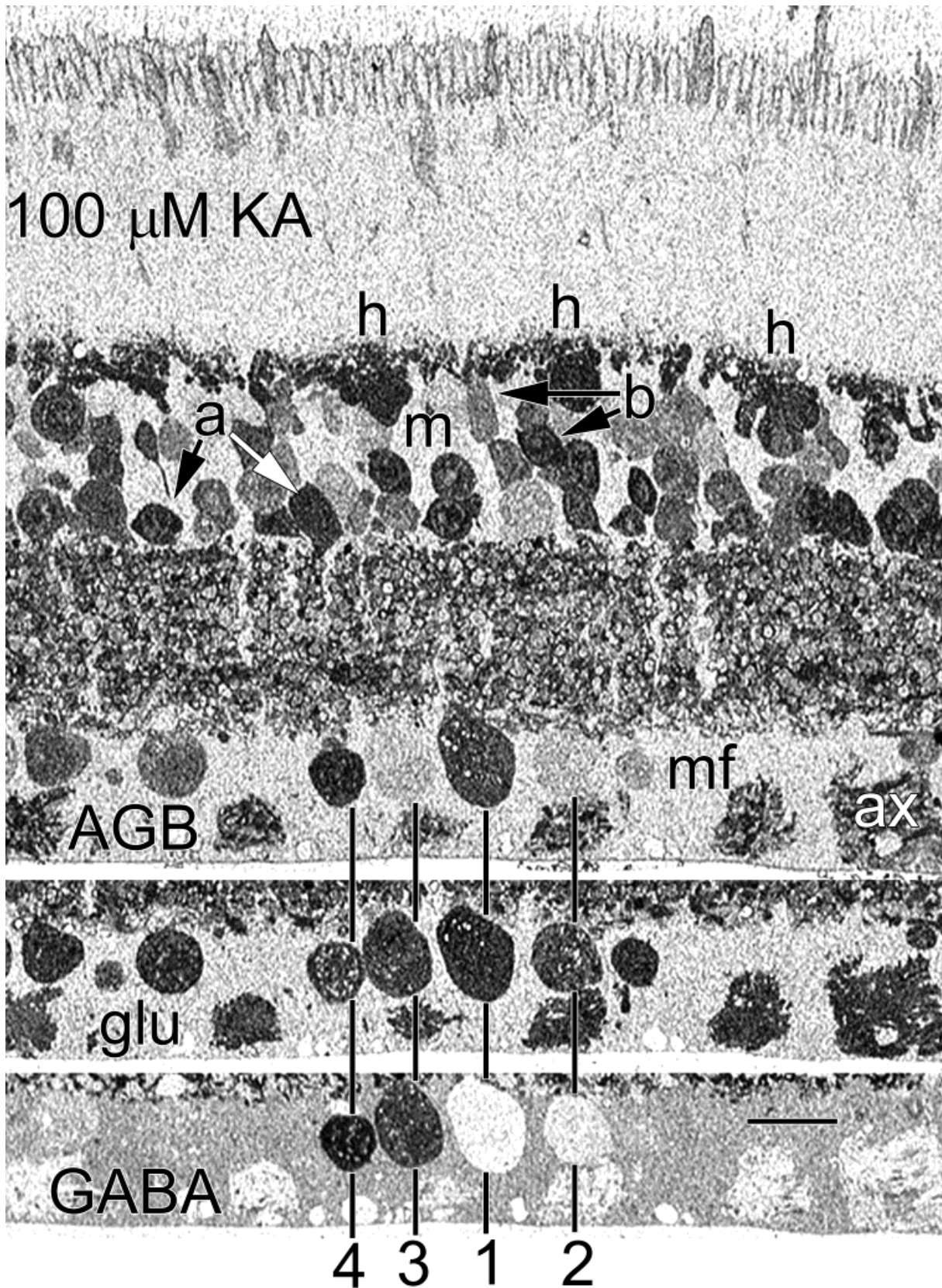


Fig. 3. 1-amino-4-guanidobutane (AGB) signals in rabbit retina after incubation in Ames medium plus 5 mM AGB in the presence of 100  $\mu\text{M}$  kainic acid (KA). Endogenous glutamate (glu) and GABA signals in the ganglion cell layer are shown as registered strips from serial sections with selected cell classes marked by vertical lines with

class labels below: 1,  $\text{E}^+$  ganglion cells with strong AGB signals; 2,  $\text{E}^+$  ganglion cells with weak AGB signals; 3,  $\text{E}^-/\gamma^+$  ganglion cells with weak AGB signals; 4,  $\gamma^+$  starburst amacrine cells with strong AGB signals. ax, Ganglion cell axon bundles. For other abbreviations, see Figure 2. Scale bar = 20  $\mu\text{m}$ .

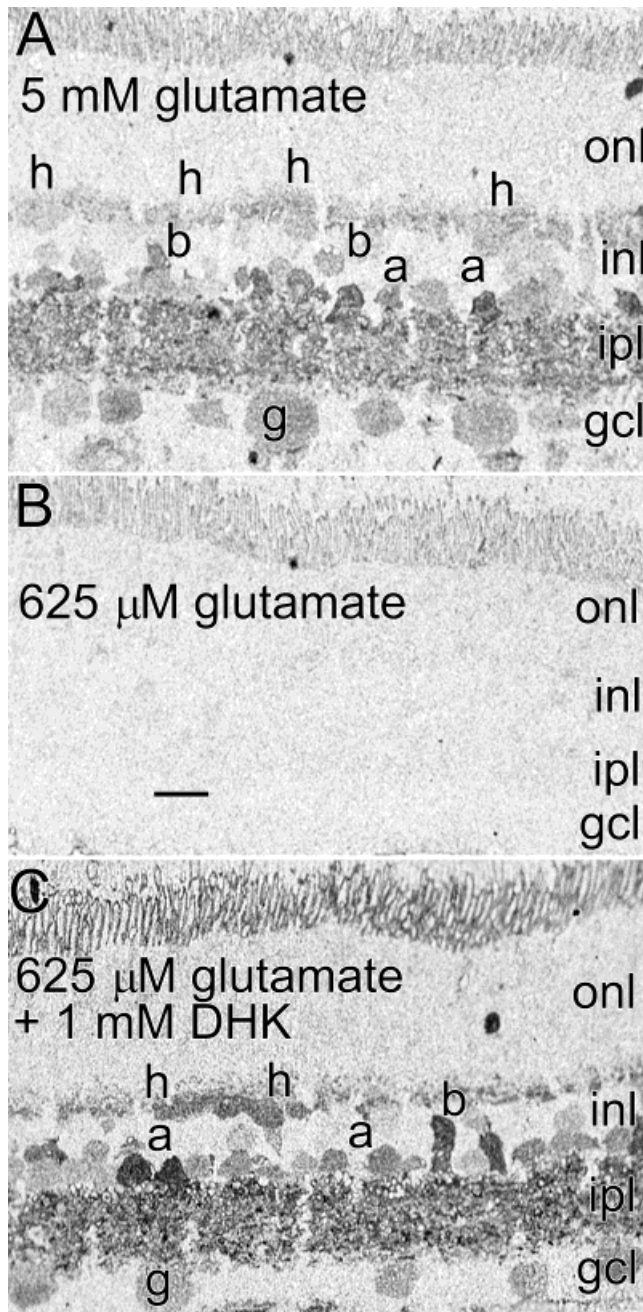


Fig. 4. 1-amino-4-guanidobutane (AGB) signals in rabbit retina after incubation in control Ames medium plus 5 mM AGB in the presence of 5 mM glutamate (A), 625  $\mu$ M glutamate (B), and 625  $\mu$ M glutamate plus 1 mM dihydrokainate (DHK; C). High glutamate doses are required to activate AGB permeation, and submillimolar doses (B) are completely ineffective. However, the glutamate transport antagonist DHK potentiates the effectiveness of glutamate in activating AGB permeation. Scale bar = 20  $\mu$ m.

dose-response stack viewed in a single 250-nm section. The minimum visual detectable threshold for KA activation was 1  $\mu$ M (not shown), in which faint bistratified strips of label appeared in the inner plexiform layer and became distinctive, and strong bistratified laminar responses were seen at 6  $\mu$ M KA. As the dose was increased, the bistrati-

fied response appeared to saturate at about 30  $\mu$ M, and other responsive elements began to fill in the gaps in the inner plexiform layer over the 63–125  $\mu$ M KA range. These patterns are shown in more detail as response amplitude profiles of AGB signal strength across the inner plexiform layer (Fig. 6). The initial bistratified responses are distinct at 6  $\mu$ M KA, centered at levels 20 and 70 of the inner plexiform layer, and appear to have saturated by 30  $\mu$ M KA. KA-induced responses of other cellular elements have a higher response threshold, are roughly half saturated by 30  $\mu$ M KA, and require between 63  $\mu$ M and 125  $\mu$ M KA to reach response saturation and fill in the regions between the bistratified bands.

AMPA-activated responses (not shown in Fig. 5) were similar in form overall to those induced by KA, especially with the appearance of bands at levels 20 and 70 of the inner plexiform layer near threshold and some filling in of the inner plexiform layer at progressively stronger doses. The threshold dose of AMPA was at least threefold lower than KA ( $\approx$ 300 nM), but even saturating doses of AMPA did not activate as many profiles as KA. Furthermore, the AGB signal in many profiles in the inner plexiform layer remained low even at saturating AMPA levels.

NMDA evoked a different pattern of AGB signals in the inner plexiform layer than either AMPA or KA (Fig. 5), indicating that cells most responsive to NMDA are a different population than those most responsive to AMPA/KA. The NMDA response exhibited a threshold of about 100  $\mu$ M, saturated between 1,000  $\mu$ M and 3,000  $\mu$ M, involved fewer cells, and displayed a characteristic weak trilaminar profile. The key features of the NMDA response are broad bands centered around levels 10, 40, and 65 of the inner plexiform layer; a relative insensitivity at level 20 (the most AMPA/KA-sensitive region) that fills in rather slowly; and a region spanning levels 90–100 in which very few NMDA-responsive profiles are present (Fig. 6). The pattern of NMDA activation in  $Mg^{2+}$ -free medium (four NMDA series at 4–5 concentrations each; not shown) was similar to that induced in normal Ames medium, suggesting that most endogenous excitations in the intact *in vitro* retina are capable of overcoming voltage-dependent  $Mg^{2+}$  block. Detail analyses of  $Mg^{2+}$ -free NMDA responses are not presented here, but no evidence of horizontal cell activation was seen at any NMDA dose in the presence or absence of  $Mg^{2+}$ . Starburst amacrine cells did show an enhanced AGB signal after exposure to NMDA doses that normally evoked little response. Weak bipolar cell signals emerged in some  $Mg^{2+}$ -free preparations, and the mechanism has not yet been resolved.

**Fractional response functions in the inner plexiform layer.** The recruitment of ligand-responsive elements can be measured as a “fractional response” of the entire bipolar, amacrine, and ganglion cell populations, defined as the area of the inner plexiform layer for which the AGB signal exceeds a criterion strength ( $GV \geq 127$  for AMPA/KA/NMDA [Fig. 7];  $GV \geq 87$  for glutamate [Fig. 8]). The dynamic range of the fractional response function represents the ligand concentrations required to recruit a full population of responses through a mechanism and is delimited by the cumulative response ranges of the most and least sensitive cell types. If all cells possess identical types of AMPA/KA receptors, then the effective dose ranges of the fractional response function of the inner plexiform layer and responses of individual cell types should be identical. This is clearly not so. For example, total inner

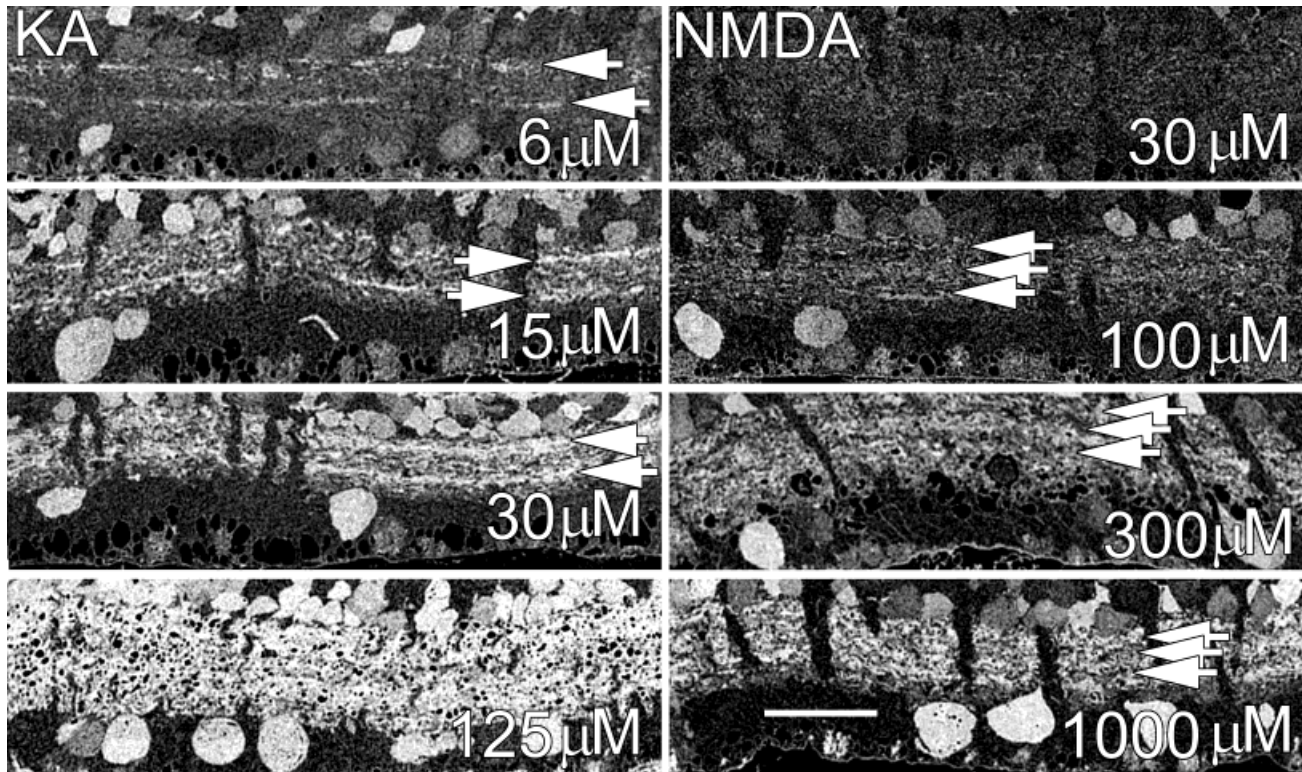


Fig. 5. Anatomical dose response series for the inner plexiform layer activated by KA and NMDA. **Left:** 1-amino-4-guanidobutane (AGB) signals induced by kainic acid (KA) are aligned top to bottom with increasing micromolar dose concentrations. All images are intensity scaled; the top and bottom of each frame is delimited by the amacrine and ganglion cell layers, respectively. Only four of six response images are shown. Distinctive, bistratified signals induced by KA are marked by arrowheads and represent levels 20 (top) and 70

(bottom) of the inner plexiform layer. Eventually, the entire inner plexiform layer fills with AGB signals at 125  $\mu\text{M}$  KA. **Right:** The pattern of NMDA-evoked responses is subtly different from KA, with a threshold of about 100  $\mu\text{M}$ , eventually resolving three distinct response peaks. Weak, tristratified signals evoked by 300  $\mu\text{M}$  NMDA are marked by arrowheads and represent levels 10, 40, and 65 of the inner plexiform layer. Responses saturate between 1 mM and 3 mM NMDA. Scale bar = 20  $\mu\text{m}$ .

plexiform layer fractional responses (Fig. 7) and starburst amacrine cell responses inferred from inner plexiform layer strata (Figs. 5, 9) measured by AGB signals both exhibit visual KA thresholds of about 1–3  $\mu\text{M}$ , but starburst amacrine cells apparently saturate at about 15–30  $\mu\text{M}$ , when the fractional response has achieved only 20% of its magnitude. The fractional response function proves, as response curves for individual cell types cannot, that some unknown cell types do not saturate until doses of 125  $\mu\text{M}$  or greater are applied.

AMPA is a much more potent agonist than KA, because lower concentrations were required to activate population responses (Fig. 7); however, AMPA does not evoke the same fractional response as KA. Glutamate is an ineffective ligand in two senses (Fig. 8): First, it evokes very weak responses and, at saturation, recruits only about 4% of the elements in the inner plexiform layer without adjustment of the response criterion. The criterion was adjusted to  $\text{GV} = 87$  (a 0.3 log unit decrease in detection threshold) to estimate ligand sensitivities, although this necessarily increased the variances of individual measurements. Second, after shifting the criterion, it was possible to demonstrate that the effectiveness of glutamate was strongly impacted by glial glutamate transport. The visual response threshold was shifted from  $>1$  mM to 125–200  $\mu\text{M}$  glutamate in the presence of the glutamate transport inhibitor DHK.

The fractional response function allows an estimation of the proportion of neurons responding to a nondesensitizing agonist. The fractional response evoked by KA accounts for about 55% of the inner plexiform layer, indicating that large portions of all cell types have AMPA/KA-driven receptors. However, Müller cells comprise  $36\% \pm 3.5\%$  of the volume of the inner plexiform layer, as determined from 18 fields of D-aspartate labeling (see Marc et al., 1995). After correction for the glial compartment,  $\approx 86\%$  of the neuronal volume of the inner plexiform layer appears to be KA responsive. These data imply that different cell types contributing to the inner plexiform layer must have different affinities for KA and form different fractions of the responsive population. AMPA is a much more effective ligand than KA and exhibited visual threshold responses at about 300 nM. However, maximal AMPA-activated AGB signals are weaker than those activated by KA, only driving about 15% of the inner plexiform layer to criterion responses. These response differences are likely due to fast desensitization of AMPA responses and perhaps to different final conductances accessed by different ligands. NMDA-responsive elements exhibited a dynamic range of 100–3,000  $\mu\text{M}$  but saturated at only 25–30% of the inner plexiform layer area. Because NMDA responses do not desensitize significantly, and all apparently reach the criterion GV of 127, only 40–50% of the neuronal profiles comprising the inner plexiform layer

appear to possess NMDA receptors that are activated in the presence of  $Mg^{2+}$ .

The fractional response function also demonstrates the pharmacologic specificities of the signal monitored by AGB permeation. The AMPA receptor antagonist CNQX (5–20  $\mu M$ ) competitively attenuated all KA-induced responses (Fig. 7). Furthermore, NBQX blocked responses to 30  $\mu M$  KA with an  $IC_{50}$  of  $\approx 5 \mu M$  (not shown), and 2.5  $\mu M$  NBQX shifted the responses to AMPA by about 1.3 log units. The competitive NMDA receptor antagonist D-AP7 was able to induce a 0.5 log unit shift in the NMDA response curve at 100  $\mu M$  and a greater than 1.0 log unit shift at 300  $\mu M$ , but

it was totally ineffective against KA or AMPA. However, both CNQX and NBQX attenuated the maximum fractional signal induced by NMDA by at least 50% without detectably shifting the dose-response curve. Part of this effect is associated with  $Mg^{2+}$  blockade, which will be described in a later report, and suggests that endogenous glutamate activation of AMPA/KA receptors is a major mechanism for overcoming  $Mg^{2+}$  blockade in our preparations (see Diamond and Copenhagen, 1993). Overall, each ligand elicits a different pattern of responses in terms of 1) the variety of cell types activated, 2) the laminar pattern of activation in the inner plexiform layer, 3) the pharmacologic specificity of the activation, and 4) the different fractions of the neuronal population activated.

**Dose-response functions of representative cells.** The horizontal cell population of the rabbit retina is comprised of two morphologic types that are treated as a single population, because their AMPA/KA dose-response curves are statistically indistinguishable. The KA responses of horizontal cells displayed a threshold of about 3  $\mu M$  and saturated around 63  $\mu M$  (Fig. 9). AMPA was more effective, with a threshold between 300 nm and 1  $\mu M$ . The specificity of this response for AMPA/KA receptors was demonstrated by blockade with 2.5  $\mu M$  NBQX, which resulted in a 1.6 log unit shift in the AMPA dose-response function. Thus, horizontal cells provide a quantitative comparison for other cell types. The bistratified signals arising from dendrites of starburst amacrine cells in the inner plexiform layer described in Figure 5 have much lower thresholds and saturation values for both AMPA and KA (Fig. 9) and, thus, must have AMPA/KA receptors with higher affinities for those ligands.

#### AGB entry is not activated by cholinergic agonists, purinergic agonists, or release from inhibition

Despite the facts that many guanidinium analogues are permeable at the neuromuscular junction (Dwyer et al., 1980) and that AGB has been shown to enter cells activated by nicotinic agonists (Yoshikami, 1981), neither carbachol (62–1,000  $\mu M$ ; two series), epibatidine (2–2,000 nm; one series), nor acetylcholine (0.5–500  $\mu M$  in the presence or absence of cholinesterase inhibitors; one series

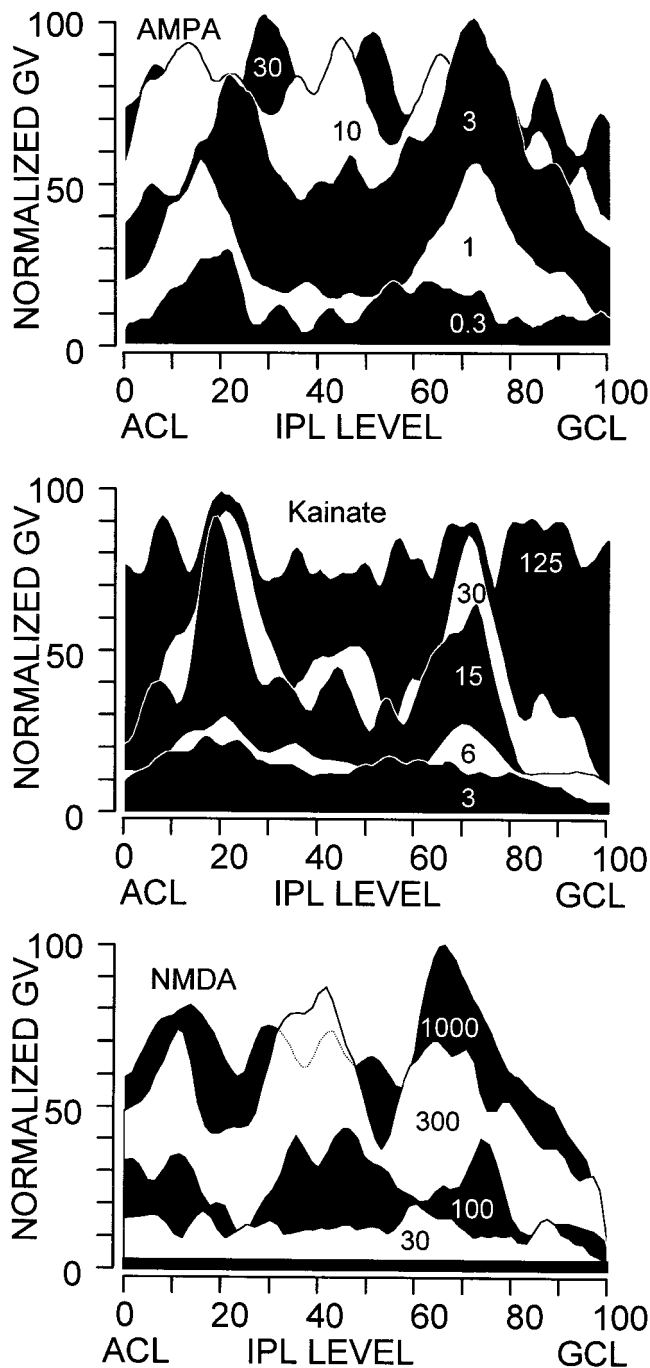


Fig. 6. Laminar response profiles for the inner plexiform layer (IPL) after activation by  $\alpha$ -amino-3-hydroxy-5-methylisoxazole-4-propionic acid (AMPA) (top), kainic acid (KA) (middle), and N-methyl-D-aspartic acid (NMDA) (bottom). The inner plexiform layer has a distinctive profile of AGB signals for each micromolar ligand dose marked on alternating black-and-white filled profiles, normalized to the maximal induced signal for each ligand. **Top:** Threshold AMPA responses are evident at 300 nm, and the most responsive regions at low doses are two levels ( $\approx 20$  and  $\approx 70$ ) between which signals accumulate slowly at higher doses. The profile at 100  $\mu M$  AMPA is omitted for clarity, because it is similar to the 30- $\mu M$  profile. **Middle:** KA response patterns are similar to AMPA responses but require higher ligand doses and are less noisy. The profile at 63  $\mu M$  KA is deleted for clarity. Levels 20 and 70 have effectively saturated at a dose of 30  $\mu M$  KA, whereas those that fill in the remainder of the inner plexiform layer have a higher saturation concentration and a lower apparent affinity for KA. **Bottom:** The pattern of NMDA-evoked responses is subtly different from both AMPA and KA, eventually resolving three response peaks. Even after the peak signal saturates some portions of the inner plexiform layer, especially levels 90–100, they never develop strong responses. GV, gray value; ACL, amacrine cell layer.

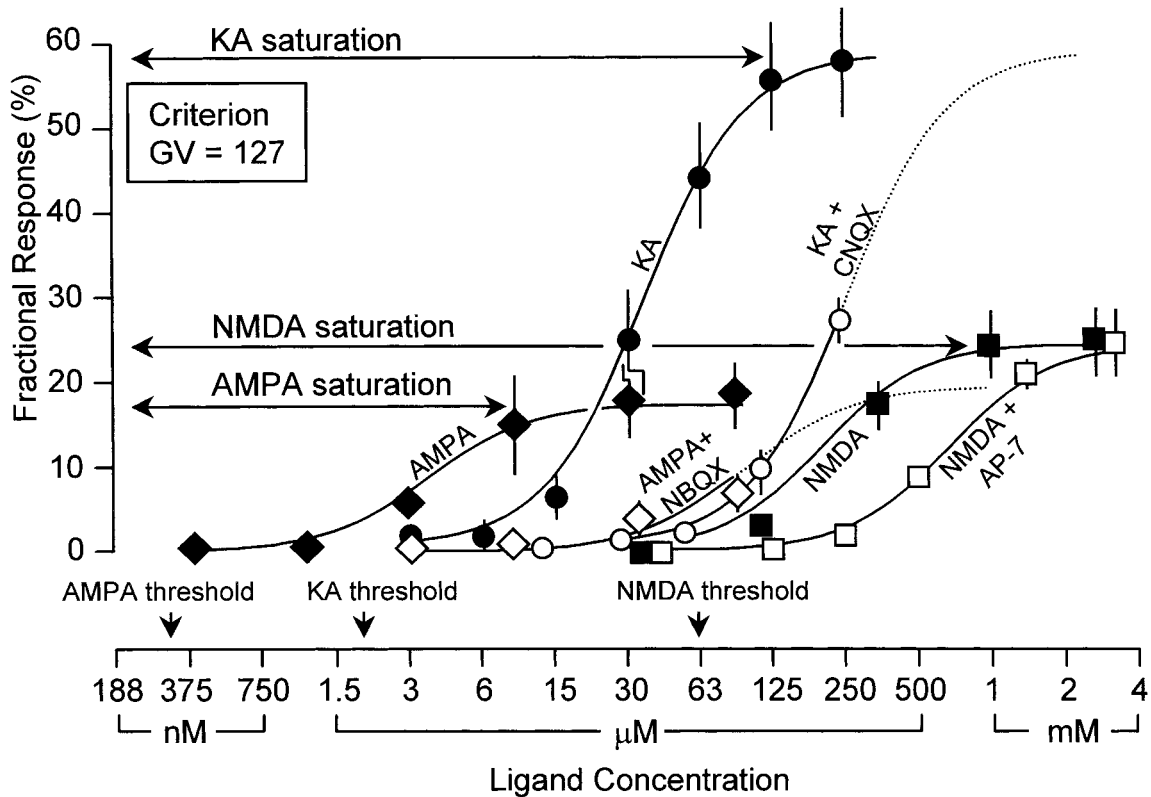


Fig. 7. Fractional response curves for the rabbit retinal inner plexiform layer as a function of log glutamate receptor agonist concentration in the absence or presence of antagonists. The response at each condition is the fractional area of the inner plexiform layer reaching the criterion gray value (GV) of 127. Each point is the mean  $\pm$  1 S.D. of 10–15 vertical section samples, each  $\geq 100$   $\mu\text{m}$  long, and all points on a single curve are from one retina and points without error bars have S.D.s smaller than the symbol. Curves were visually fitted with a full cooperativity Hill function. The  $\alpha$ -amino-3-hydroxyl-5-methylisoxazole-4-propionic acid (AMPA) fractional response (solid diamonds) was activated around 300 nM, saturated by 30  $\mu\text{M}$ , comprised just below 20% of the inner plexiform layer area, and was shifted over 1 log unit by 2.5  $\mu\text{M}$  1,2,3,4-tetrahydro-6-nitro-2,3-

dioxobenzo[*f*]quinoxaline-7-sulfonamide (NBQX; open diamonds) but was unaffected by 2-amino-7-phosphonoheptanoate (AP-7; not shown). The kainic acid (KA) fractional response (solid circles) was activated around 1  $\mu\text{M}$ , saturated by 125  $\mu\text{M}$  at 60% of the inner plexiform layer, and was shifted almost 1 log unit by 20  $\mu\text{M}$  6-cyano-7-nitroquinoxaline-2,3,-dione (CNQX; open circles) but was unaffected by AP-7 (not shown). The N-methyl-D-aspartic acid (NMDA) response (solid squares) was activated around 63  $\mu\text{M}$ , saturated by 1 mM at 25% of the inner plexiform layer area, and was shifted about 0.5 log units by 100  $\mu\text{M}$  AP-7 (open squares). The half-saturation value of the NMDA response was unaffected by NBQX/CNQX, but both antagonists depressed the NMDA signal (not shown).

each) activated any detectable signals. This may have been due to rapid desensitization of acetylcholine receptors, cholinergic blockade associated with guanidinium analogues (Loring, 1990), or the fact that AGB may not permeate retinal acetylcholine-gated channels. This lack of signaling demonstrates that the KA- or AMPA-induced response patterns reported here do not represent secondary activations of target cells after chronic depolarization of starburst amacrine cells, which comprise the known cholinergic amacrine cell group in rabbit retina (Masland and Mills, 1979; Masland and Tauchi, 1986; Vaney, 1990).

ATP activates nonselective  $P_{2X}$  cation channels in a variety of cell types, but did not activate any detectable AGB permeation (1–1,000  $\mu\text{M}$ ; two series). The application of broad-spectrum blockers of inhibitory neurotransmission (picrotoxin: 5  $\mu\text{M}$ , 50  $\mu\text{M}$ , and 500  $\mu\text{M}$ ; two series; strychnine: 2  $\mu\text{M}$ , 20  $\mu\text{M}$ , and 200  $\mu\text{M}$ ; two series) evoked no AGB permeation, suggesting that endogenous glutamate release associated with release from inhibition (see, e.g., Critz and Marc, 1992) does not result in channel opening sufficient to be detected by using this acute protocol.

## Artifacts

The AGB mapping technique is sensitive to neuronal/glia cytopathology. In mechanically damaged regions of tissue, uncontrolled AGB labeling can occur, involving Müller cells and both rod and cone photoreceptors (Fig. 10) and often sparing neurons. There are at least three possible mechanisms for such labeling. 1) Cell rupture can expose the cytosolic matrix to which AGB can be fixed. 2) Trauma can evoke release of lytic enzymes that might perforate neighboring cells, forming channels through which AGB could enter. 3) Stretch could activate nonselective cation channels (Puro, 1991). The latter is a plausible explanation, because glutamine and taurine levels remain high in AGB-labeled Müller cells, implying that large membrane perforations are not present, and because trauma spares nearby neurons (Fig. 10A,B). Coupling among Müller cells, normally thought to be rather weak (Robinson et al., 1993), may increase under trauma and lead to patches of labeled cells with irregular borders. Whatever the mechanism, the appearance of patches of (Fig. 10A) or single (Fig. 10B) AGB-labeled Müller cells is a

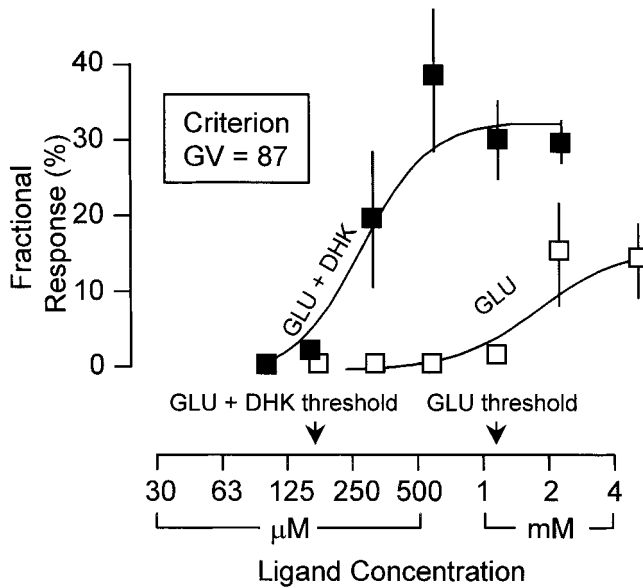


Fig. 8. Fractional response curves for the rabbit retinal inner plexiform layer as a function of log glutamate (GLU) concentration in the absence (open squares) and presence (solid squares) of dihydrokainate (DHK). The function for glutamate alone was activated at  $\approx 1$  mM and appeared saturated by 4 mM. The addition of 1 mM DHK enhanced the effectiveness of glutamate roughly eightfold, shifting the threshold to  $\approx 200$   $\mu$ M, with saturation between 625  $\mu$ M and 1 mM at over one-third of the inner plexiform layer area.

sign of local tissue trauma. Patches of heavily labeled rods and cones likely arise from damage to outer segments, allowing AGB entry (Fig. 10C). Another anomalous signal is common near damaged or cut regions. Even in the absence of any stimulus, AGB signals in presumed type A horizontal cells can be observed in occasional samples (Fig. 10D). This may be due to extensive coupling through horizontal cells from a cut site in which damaged horizontal cells are heavily loaded with AGB. Spontaneous horizontal cell labeling is especially common in  $Ca^{2+}$ -free media, suggesting that AGB also may enter through hemijunctions of connexons (DeVries and Schwartz, 1992). When tissue is sectioned, it is not possible to know whether there are damaged regions nearby (Fig. 10, bottom), and the best clue to tissue integrity is the general homogeneity of response patterns.

## DISCUSSION

### AGB appears to enter neurons through ligand-gated channels, not through transporters or voltage-gated channels

The patterns of AGB labeling described here are consistent with AGB entry through permeation of ligand-gated channels. Guanidinium cations are well-known permeants of several ligand-gated channel types, and, similarly, AGB does not enter most retinal cells unless glutamatergic agonists are applied. These effects are both pharmacologically specific and quantitatively consistent with dose dependencies reported for KA, AMPA, and NMDA in electrophysiological studies. AGB apparently enters cells most effectively through nonselective ion channels gated by ionotropic glutamate receptors. No evidence of significant

entry through voltage-activated channels could be deduced from  $K^+$  depolarization or  $Ca^{2+}$  channel-blocking experiments. Similarly, conventional symport processes likely are not involved, because most  $Na^+$ -dependent amino acid/amine (Shank et al., 1987) and dicarboxylic acid (Ganapathy et al., 1988) transport processes are attenuated by  $Na^+$  substitutes (Wright et al., 1996), and such replacements had no impact on ligand-activated labeling.

Although ligand-activated AGB permeation continues unabated under conditions that suppress most known  $Na^+$ -dependent transporters, novel inward-directed transporters activated by depolarization might mediate AGB entry into neurons. However, the ineffectiveness of elevated extracellular  $K^+$  would seem to exclude such a process. Furthermore, the transfer rates of channels ( $10^6$ – $10^7$  ions/second) vastly exceed those of transporters ( $10^3$ – $10^4$  molecules/second), and, even if AGB were only 10% as permeant as sodium and were present at 5 mM in normal Ames medium, a single channel could still mediate 3–300 times the flux of single transporter. We do not know the permeability of any glutamate-activated channel to AGB, however, similar to other guanidinium cations, it may exceed that of  $Na^+$  (Hille, 1992), and single-channel AGB fluxes would then outpace most transporters by three orders of magnitude. This is not a trivial point, because even the amino acid arginine, a natural guanidinium cation (AGB with an additional carboxyl group), can permeate NMDA and many AMPA/KA receptor systems as well (Marc, 1997). One study of arginine transport in brain synaptosomes reported an anomalous dependence on  $Na^+$  concentration, actually increasing as  $Na^+$  levels decreased, which was interpreted as activation of the transporter (Aldridge and Collard, 1996). The data presented here suggest that measurements of transport may actually be corrupted by channel-permeation effects.

### AMPA and KA responses

AGB permeation patterns induced by KA and AMPA are similar but not identical. KA preferentially activates AMPA and KA receptors and is nondesensitizing at AMPA receptors but not KA receptors (Lerma et al., 1993; Paternain et al., 1995). Conversely, KA desensitizes more rapidly at presumed KA receptors than AMPA. Responses evoked by KA may derive largely from sustained AMPA receptor activations, permitting maximal AGB entry. However, true KA receptors are also present, because GluR5 mRNA signals have been reported in the rat inner nuclear layer (Hughes et al., 1992; Müller et al., 1992), and various patterns of GluR6 or GluR7 immunoreactivity appear in mammalian horizontal cells (Morigawa et al., 1995; Brandstätter et al., 1996). This may explain the fact that AMPA seems to be as potent for activating AGB permeation in horizontal cells as KA (Figs. 2, 3), whereas it seems to be far less potent than KA for activating bipolar cells. However, horizontal cells also are reported to express AMPA receptor subunits (Qin and Pourcho, 1996), and, because certain hippocampal neurons appear to express independent, functional KA and AMPA receptor populations in the same postsynaptic dendrites (Roche and Huganir, 1995), a nondesensitizing action of KA at AMPA receptors and a weak desensitizing action of AMPA at KA receptors on the same cell may lead to a similarly strong AGB signal through independent paths.

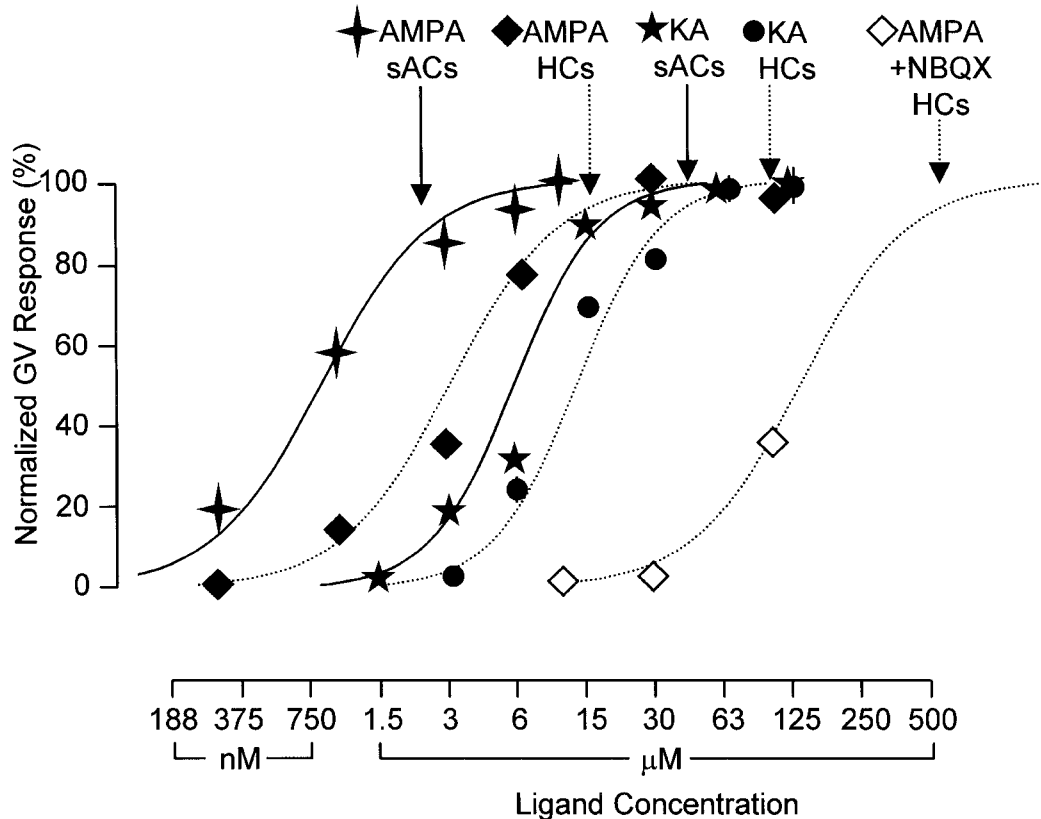


Fig. 9. Normalized dose-response curves comparing horizontal cells (HCs) and the inner plexiform layer strata (presumed to arise from starburst amacrine cells; sACs) after application of  $\alpha$ -amino-3-hydroxy-5-methylisoxazole-4-propionic acid (AMPA) and kainic acid (KA). Both populations have higher AMPA and KA sensitivities than the bulk fractional response curves. Starburst amacrine cell AMPA

(four-point stars) and KA (five-point stars) responses are activated at lower doses relative to horizontal cell AMPA (solid diamonds) and KA (solid circles) responses. The finding that horizontal cell responses arise from activation of bona fide AMPA/KA receptors is supported by the apparent competitive antagonism of AMPA responses by 2.5  $\mu$ M NBQX (open diamonds).

Detailed analyses of bipolar and amacrine cell subpopulations are beyond the scope of this report. However, mixed patterns of bipolar cell responses were induced by KA and AMPA (Figs. 2, 3), as expected from electrophysiological data showing that OFF-center bipolar cells preferentially bear classical ionotropic GluRs and are KA sensitive, whereas ON-center bipolar cells employ metabotropic GluRs and are largely KA insensitive (Slaughter and Miller, 1981, 1983b; Karschin and Wässle, 1990; Yamashita and Wässle, 1991; de la Villa et al., 1995; Euler et al., 1996; Hartveit, 1996, 1997; Sasaki and Kaneko, 1996).

### NMDA responses

NMDA-activated responses are largely restricted to amacrine and ganglion cells, and these data will be considered in more detail in a later paper. Consistent with the findings of Massey and Miller (1987), 30–3,000  $\mu$ M NMDA did not activate any horizontal cells in normal or  $Mg^{2+}$ -free Ames medium. Similarly, no distinct bipolar cell responses emerged in the presence of  $Mg^{2+}$ , but weak and variable signals did emerge in  $Mg^{2+}$ -free conditions, suggesting that low levels of NMDA receptor expression may occur in some bipolar cells. This possibility is supported by evidence of weak NMDA activation of currents in rod bipolar cells (Karschin and Wässle, 1990), but not cone bipolar cells (Hartveit, 1996), by expression of the NMDA

receptor subunits in rod bipolar cells (Hughes, 1997; Wenzel et al., 1997), and by subunits NR1/NR2C in probable bipolar cells (Brandstätter et al., 1994).

### Agonist sensitivities measured by AGB signals

AGB signals closely match electrophysiological sensitivity to agonist application. Vertebrate horizontal cell thresholds for KA are reported to range from 2–3  $\mu$ M in fishes (Ariel et al., 1984; Zhou et al., 1993) to 15  $\mu$ M in rabbits (Bloomfield and Dowling, 1985a). The data reported here reveal horizontal cell thresholds of  $\approx$ 3  $\mu$ M in rabbit and suggest that the threshold determinations of Bloomfield and Dowling are elevated for unknown reasons. The saturation doses are similar, however, with AGB responses saturating at  $\approx$ 63  $\mu$ M KA and voltage responses at 75  $\mu$ M (Bloomfield and Dowling, 1985a). Starburst amacrine cells had KA thresholds close to 1  $\mu$ M, were strongly activated at 6  $\mu$ M KA (a dose that evoked little responsiveness in most other retinal neurons), and were saturated near 15  $\mu$ M KA, virtually identical to values reported for KA-activated [ $^{14}$ C] acetylcholine release from rabbit starburst amacrine cells (Linn et al., 1991). Most other cells required more than 6  $\mu$ M KA/1  $\mu$ M AMPA to display threshold responses, and most were not saturated by 30  $\mu$ M KA/3  $\mu$ M AMPA. Thus, the AMPA/KA receptors expressed by most cell types

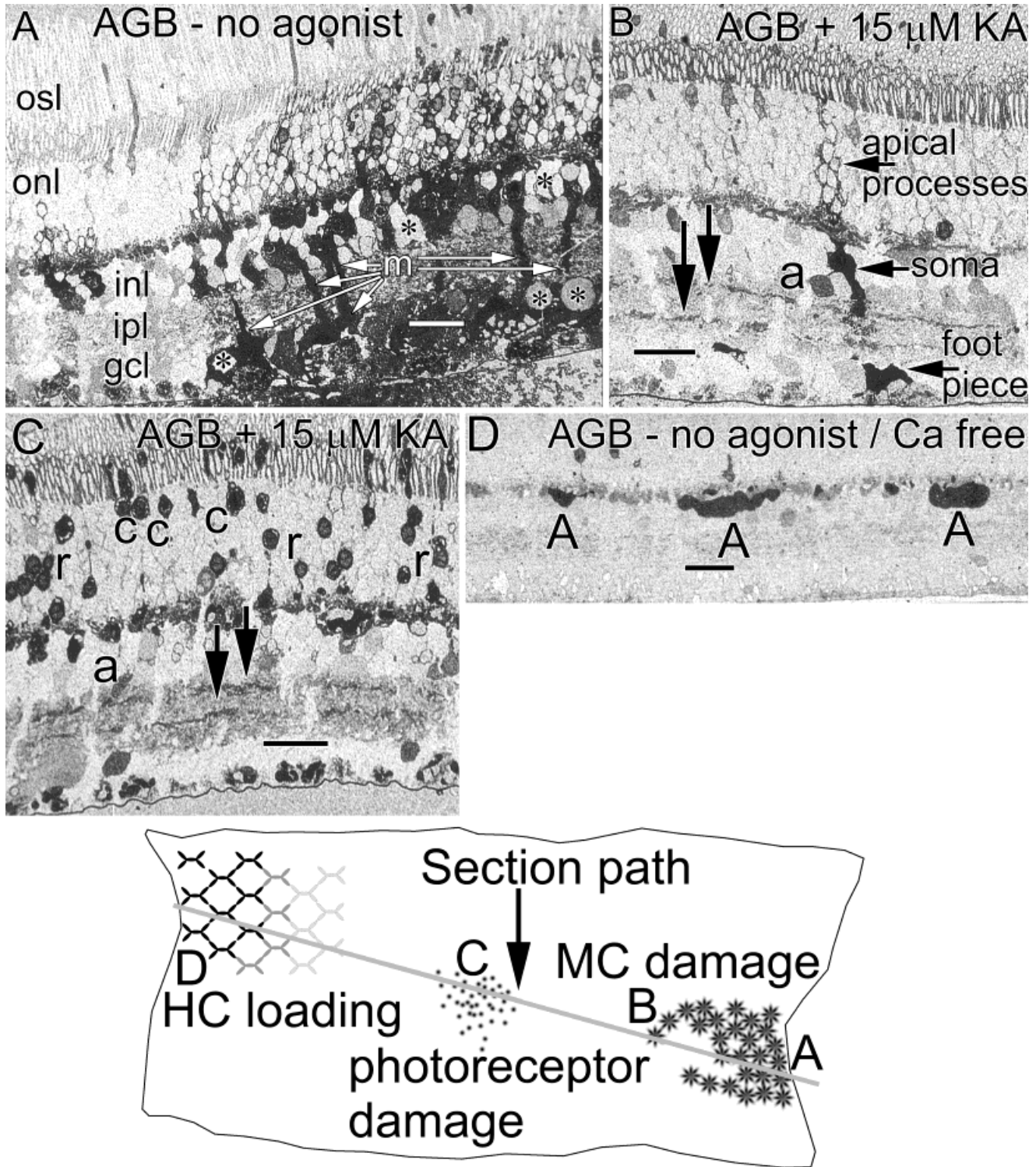


Fig. 10. Damage artifacts associated with the 1-amino-4-guanidobutane (AGB) technique. **A:** AGB signals of damaged retina within 50  $\mu\text{m}$  of the edge of a retinal chip in the absence of agonist. Trunks of Müller cells (m) displaying AGB signals surround nonresponsive neurons (asterisks) in the ganglion and inner nuclear layers. osl, Outer segment layer. **B:** An isolated AGB-labeled Müller cell in a preparation activated by 15  $\mu\text{M}$  kainic acid (KA) also displaying bistratified, responsive strata (arrows). **C:** Patches of rod (r) and cone (c) damage in

a preparation activated by 15  $\mu\text{M}$  KA also displaying bistratified, responsive strata (arrows). **D:** Type A horizontal cell (A) AGB signals incurred during incubation in  $\text{Ca}^{2+}$ -free medium. **Bottom:** Schematic interpretation of these images as a single section path through the middle and fringes of damaged neural retina, patches of mechanically damaged photoreceptors, and sheets of coupled type A horizontal cells. MC, Müller cell. Scale bars = 20  $\mu\text{m}$ .

cannot be equivalent to those on starburst amacrine cells. Although type A and type B horizontal cells differ in dendritic/axonal architecture (Dacheux and Raviola, 1982), horizontal cell AGB signals appeared homogeneous at a given KA dose, suggesting that ionotropic glutamate receptors on both cone-driven somata and rod-driven axon terminals behave similarly (cf. Massey and Miller, 1987). The fractional recruitment curves give glutamate response thresholds of  $\approx 1$  mM or greater for all responsive cells, identical to results obtained for individual neurons in intact retinas across many species and in rabbit in particular (Bloomfield and Dowling, 1985a,b). The glutamate transport antagonist DHK shifts the threshold response to below 200  $\mu$ M, similar to the effect of the competitive transport agonist D-aspartate on goldfish horizontal cells (Ishida and Fain, 1981). Finally, threshold NMDA responses appear to be about 30–60  $\mu$ M based on fractional recruitment curves and are reported to be around 100  $\mu$ M in electrophysiological measures (Massey and Miller, 1990) and 30  $\mu$ M for NMDA-activated [ $^{14}$ C] acetylcholine release (Linn and Massey, 1991) in the intact rabbit retina. However, thresholds of  $\approx 1$   $\mu$ M NMDA have been obtained by whole-cell current measurements in ganglion cells enzymatically isolated from the goldfish retina (Yazejian and Fain, 1992). The inability of the AGB method to uncover NMDA-evoked responses at 1  $\mu$ M in rabbit retina cannot be attributed to its insensitivity, because KA and AMPA thresholds determined by AGB signals clearly match electrophysiologic data. The physiology of the NMDA mechanism in the two preparations must underlie this large difference.

### What do differences in AGB responses mean?

**Affinity differences.** The affinities of various cells for AMPA/KA cannot be equivalent and must vary across cell types. For example, starburst amacrine cells become activated long before any ganglion, horizontal, or other amacrine cell type and appear to saturate at doses at which remaining elements of the inner plexiform layer are far from saturation (Figs. 7, 9). The apparent affinities of recombinant AMPA receptors vary according to subunit composition (Arvola and Keinänen, 1996; Hennegriff et al., 1997), and, although little is known of mixed subunit properties, it is probable that major differences in the apparent dose responsiveness observed by AGB permeation reflect affinity differences in subunits. A clear limitation of both conventional electrophysiologic methods and AGB permeation is the fact that bath-applied agonists will activate both synaptic and nonsynaptic ionotropic receptors. To the extent that a given cell type expresses similar subunits and receptor types at both synaptic and nonsynaptic sites, differences in apparent affinity across all cell types (see, e.g., Fig. 9) should still be valid. However, unknown fractions of the absolute response magnitudes for various cell types may derive from nonsynaptic activations.

**Channel permeability differences.** The amount of AGB entering a cell at any time is the product of open channel number and channel permeability, values that cannot be dissociated at present, even at saturation. The permeability of each subunit type to AGB is not known. Organic cation probes with different sizes can differentiate permeability and channel number (Marc, 1997). The relative permeabilities of glutamate-gated horizontal cell channels cannot be identical to those of various OFF-center

bipolar cells based on concurrent arginine and AGB permeation experiments (Marc, 1997 and unpublished data). Thus, cells with extremely large channels may possess larger maximal currents (depending on other electromorphologic factors), even if their affinities for glutamate match other cell types.

**Temporal differences in receptor/channel complexes.** Channel desensitization has not been demonstrated quantitatively with the AGB method in this report, although differences in responses to AMPA and KA likely arise from desensitization. In principle, it should be quite detectable, but the variation in desensitization extent and drug responsiveness across cell types is dramatic in recombinant and intact systems (Johansen et al., 1995; Partin et al., 1996; Washburn et al., 1997). Although it may be simple to detect in single cells (Mosbacher et al., 1994), complex populations pose a greater analytical challenge. A cocktail of desensitization blockers may be necessary to reveal which cells are dominated by AMPA receptors regardless of splice variant. This type of experiment is complicated by the growing evidence that KA receptors are coexpressed widely with AMPA receptors (Brandstätter et al., 1994), some form being present in virtually every cell type.

**Circuitry.** The data reported here suggest that the acute protocol employed to gauge ligand-gated AGB responses is insensitive to most polysynaptic effects in the sense that GABAergic, glycinergic, and cholinergic agents reveal no intrinsic responses or any changes in responses to glutamate agonists. Longer incubation times or other parametric variations may make the method more sensitive to intrinsic circuitry effects.

### Müller cells

NMDA-gated currents have been reported in mammalian Müller cells (Uchiyori and Puro, 1993; Puro et al., 1996) as well as NMDA/AMPA activation of Müller cell transcription factors (Lopez-Colomé et al., 1995). There is no doubt that, under any conditions used here, Müller cells show no significant AGB permeation after NMDA, AMPA, KA, or glutamate exposure. This suggests that the magnitudes of currents evoked by agonists in neurons are far larger than those of Müller cells and that, under any conditions, native Müller cells probably display miniscule currents through glutamate-activated NMDA receptors. The neurons of the inner retina serve as a powerful control, demonstrating that Müller cells are the least responsive element of the inner retina to glutamatergic ionotropic activation. Trauma apparently can activate a permeation mechanism that is as effective as a ligand-gated channel, showing that it is possible to generate large AGB signals in Müller cells.

### AGB mapping and its applications

Guanidinium analogues have been employed as sieving agents in biophysical analyses of channel dimensions for nearly 30 years. Immunodetection of the guanidinium analogue AGB provides physiologic access to permeation events, regardless of cell size or numbers, and can be used as a general probe in brain slices, isolated ganglia, and cultured neurons. In addition to permeating cone photoreceptors, AGB permeates olfactory receptor neurons and neuromast organ cells in zebrafish (M. Michel, personal communication), suggesting that AGB may be a useful survey tool for other types of channels. However, no evidence of entry through cyclic GMP-gated channels has

been achieved to date. Arginine is a channel-permeant probe with a different labeling profile (Marc, 1997), and different organic cations potentially can map cells that express channels of different maximal pore sizes. Finally, AGB also can be employed *in vivo* in the vitreous chamber of the eye as a probe of endogenous glutamate-mediated channel activation under natural stimulus conditions (Marc, unpublished data).

## ACKNOWLEDGMENTS

This work was supported by a Research to Prevent Blindness Jules and Doris Stein Professorship.

## LITERATURE CITED

- Aldridge CR, Collard KJ. 1996. The characteristics of arginine transport by rat cerebellar and cortical synaptosomes. *Neurochem Res* 21:1539–1546.
- Ames A III, Nesbitt FB. 1981. *In vitro* retina as an experimental model of the central nervous system. *J Neurochem* 37:867–877.
- Ariel M, Lasater EM, Mangel SC, Dowling JE. 1984. On the sensitivity of H1 horizontal cells of the carp retina to glutamate, aspartate and their agonists. *Brain Res* 295:179–183.
- Arvola M, Keinänen K. 1996. Characterization of the ligand-binding domains of glutamate receptor GluR-B and GluR-D subunits expressed in *Escherichia coli* as periplasmic proteins. *J Biol Chem* 271:15527–15532.
- Balasubramanian S, Lynch JW, Barry PH. 1995. The permeation of organic cations through cAMP-gated channels in mammalian olfactory receptor neurons. *J Membrane Biol* 146:177–191.
- Berdeu D, Puech R, Loubatières-Mariani M-M, Bertrand G. 1996. Agmatine is not a good candidate as an endogenous ligand for imidazole sites of pancreatic B cells and vascular bed. *Eur J Pharmacol* 308:301–304.
- Bloomfield SE, Dowling JE. 1985a. Roles of aspartate and glutamate in synaptic transmission in rabbit retina. I. Outer plexiform layer. *J Neurophysiol* 53:699–713.
- Bloomfield SE, Dowling JE. 1985b. Roles of aspartate and glutamate in synaptic transmission in rabbit retina. II. Inner plexiform layer. *J Neurophysiol* 53:714–725.
- Brandstätter JH, Hartveit E, Sassoe-Pognetto M, Wässle H. 1994. Expression of NMDA and high-affinity kainate receptor subunit mRNAs in the adult rat retina. *Eur J Neurosci* 6:1100–1112.
- Brandstätter JH, Koulen P, Wässle H. 1996. Selective synaptic distribution of kainate receptor subunits in the two plexiform layers of the rat retina. *J Neurosci* 17:9298–9307.
- Cohen ED, Miller RF. 1994. The role of NMDA and non-NMDA excitatory amino acid receptors in the functional organization of primate retinal ganglion cells. *Visual Neurosci* 11:317–322.
- Cohen ED, Miller RF. 1995. Quinoxalines block the mechanism of directional selectivity in ganglion cells of the rabbit retina. *Proc Natl Acad Sci USA* 92:1127–1131.
- Cohen ED, Zhou ZJ, Fain GL. 1994. Ligand-gated currents of alpha and beta ganglion cells in the cat retinal slice. *J Neurophysiol* 72:1260–1269.
- Critz SC, Marc RE. 1992. Glutamate antagonists that block hyperpolarizing bipolar cells increase the release of dopamine from turtle retina. *Visual Neurosci* 9:271–278.
- Dacheux RF, Raviola E. 1982. Horizontal cells in the retina of the rabbit. *J Neurosci* 2:1486–1493.
- de la Villa P, Kurahashi T, Kaneko A. 1995. L-glutamate-induced responses and cGMP-activated channels in three subtypes of retinal bipolar cells dissociated from the cat. *J Neurosci* 15:3571–3582.
- DeVries SH, Schwartz EA. 1992. Hemi-gap-junction channels in solitary horizontal cells of the catfish retina. *J Physiol* 445:201–230.
- Diamond JS, Copenhagen DR. 1993. The contribution of NMDA and non-NMDA receptors to the light-evoked input-output characteristics of retinal ganglion cells. *Neuron* 11:725–738.
- Dwyer TM. 1986. Guanidine block of single channel currents activated by acetylcholine. *J Gen Physiol* 88:635–650.
- Dwyer TM, Adams DJ, Hille B. 1980. The permeability of the endplate channel to organic cations in frog muscle. *J Gen Physiol* 75:469–492.
- Emerit MB, Riad M, Fattaccini CM, Hamon M. 1993. <sup>14</sup>C] guanidinium ion influx into Na<sup>+</sup> channel preparations from mouse cerebral cortex. *J Neurochem* 60:2059–2067.
- Euler T, Schneider H, Wässle H. 1996. Glutamate responses of bipolar cells in a slice preparation of the rat retina. *J Neurosci* 16:2934–2944.
- Evans RJ, Lewis C, Virginio C, Lundstrom K, Buell G, Suprenant A, North RA. 1996. Ionic permeability of, and divalent cation effects on, two ATP-gated cation channels (P<sub>2X</sub> receptors) expressed in mammalian cells. *J Physiol* 497:413–422.
- Ganapathy V, Ganapathy ME, Tiruppathi C, Miyamoto Y, Mahesh VB, Leibach FH. 1988. Sodium-gradient-driven, high-affinity, uphill transport of succinate in human placental brush-border membrane vesicles. *Biochem J* 249:179–184.
- Gieger JRP, Melcher T, Koh D-S, Sakmann B, Seeburg PH, Jonas P, Monyer H. 1995. Relative abundance of subunit mRNAs determines gating and Ca<sup>2+</sup> permeability of AMPA receptors in principal neurons and interneurons of rat CNS. *Neuron* 15:193–204.
- Hamana K, Niitsu M, Samejima K, Matsuzaki S. 1991. Novel polyamines in insects and spiders. *J Comp Biochem Physiol B* 100:399–402.
- Hartveit E. 1996. Membrane currents evoked by ionotropic glutamate receptor agonists in rod bipolar cells in the rat retinal slice preparation. *J Neurophysiol* 76:401–422.
- Hartveit E. 1997. Functional organization of cone bipolar cells in the rat retina. *J Neurophysiol* 77:1716–1730.
- Hennegriff M, Arai A, Kessler M, Vanderklip P, Mutneja SM, Rogers G, Neve RL, Lynch G. 1997. Stable expression of recombinant AMPA receptor subunits: binding affinities and effects of allosteric modulators. *J Neurochem* 68:2424–2434.
- Hensley SH, Yang X-L, Wu SM. 1993. Identification of glutamate receptor subtypes mediating inputs to bipolar cells and ganglion cells in the tiger salamander retina. *J Neurophysiol* 69:2099–2107.
- Hille B. 1992. Ionic channels of excitable membranes. Sunderland, MA: Sinaur Associates, Inc.
- Hughes TE. 1997. Are there ionotropic glutamate receptors on the rod bipolar cell of the mouse retina? *Visual Neurosci* 14:103–109.
- Hughes TE, Hermans-Borgmeyer I, Heinemann S. 1992. Differential expression of glutamate receptor genes (GluR 1–5) in the rat retina. *Visual Neurosci* 8:49–55.
- Ishida AT, Fain GL. 1981. D-aspartate potentiates the effects of L-glutamate on horizontal cells in goldfish retina. *Proc Natl Acad Sci USA* 78:5890–5894.
- Johansen TH, Chaudhary A, Verdoorn TA. 1995. Interactions among GYKI-52466, cyclothiazide, and aniracetam at recombinant AMPA and kainate receptors. *Mol Pharmacol* 48:946–955.
- Kalloniatis M, Fletcher E. 1993. Immunocytochemical localization of amino acid neurotransmitters in the chicken retina. *J Comp Neurol* 336:174–193.
- Karschin A, Wässle H. 1990. Voltage- and transmitter-gated currents in isolated rod bipolar cells of rat retina. *J Neurophysiol* 63:860–876.
- Kolb H, Nelson R, Mariani A. 1981. Amacrine cells, bipolar cells and ganglion cells of the cat retina. *Vision Res* 21:1081–1114.
- Kramer RH, Tibbs GR. 1996. Antagonists of cyclic nucleotide-gated channels and molecular mapping of their site of action. *J Neurosci* 16:1285–1293.
- Kuzirian AM, Meyhofer E, Hill L, Neary JT, Alkon DL. 1986. Autoradiographic measurement of tritiated agmatine as an indicator of physiologic activity in *Hermisenda crassicornis* visual and vestibular neurons. *J Neurocytol* 15:629–644.
- Lerma J, Paternain AV, Naranjo JR, Mellström B. 1993. Functional kainate-selective glutamate receptors in cultured hippocampal neurons. *Proc Natl Acad Sci USA* 90:11688–11692.
- Li G, Regunathan S, Barrow CJ, Eshraghi H, Cooper R, Reis DJ. 1994. Agmatine: an endogenous clonidine-displacing substance in the brain. *Science* 263:966–969.
- Linn DM, Massey SC. 1991. Acetylcholine release from the rabbit retina mediated by NMDA receptors. *J Neurosci* 11:123–133.
- Linn DM, Blazynski C, Redburn DA, Massey SC. 1991. Acetylcholine release from the rabbit retina mediated by kainate receptors. *J Neurosci* 11:111–122.
- Lomeli H, Mosbacher J, Melcher T, Höger T, Geiger JRP, Kuner T, Monyer H, Higuchi M, Bach A, Seeburg PH. 1994. Control of kinetic properties of AMPA receptor channels by nuclear RNA editing. *Science* 266:1709–1713.

- Lopez-Colomé AM, Murbartian J, Ortega A. 1995. Excitatory amino acid-induced AP-1 DNA binding activity in Müller glia. *J Neurosci Res* 41:179–184.
- Loring RH. 1990. Agmatine acts as an antagonist of neuronal nicotinic receptors. *Br J Pharmacol* 99:207–211.
- Marc RE. 1997. Neurochemical and glutamatergic response signatures in the retinal ganglion cell layer. *Invest Ophthalmol Vis Sci* 38:s689.
- Marc RE. 1999. Kainate activation of horizontal, bipolar, amacrine, and ganglion cells in the rabbit retina. *J Comp Neurol* 407:65–76.
- Marc RE, Liu W-LS. 1985. Glycine-accumulating neurons in the human retina. *J Comp Neurol* 232:241–260.
- Marc RE, Liu W-LS, Kalloniatis M, Raiguel S, Van Haesendonck E. 1990. Patterns of glutamate immunoreactivity in the goldfish retina. *J Neurosci* 10:4006–4034.
- Marc RE, Basinger SF, Murry RF. 1995. Pattern recognition of amino acid signatures in retinal neurons. *J Neurosci* 15:5106–5129.
- Masland RH, Mills JW. 1979. Autoradiographic identification of acetylcholine in the rabbit retina. *J Cell Biol* 83:159–178.
- Masland RH, Tauchi M. 1986. The cholinergic amacrine cell. *Trends Neurosci* 9:218–223.
- Massey SC, Miller RF. 1987. Excitatory amino acid receptors of rod- and cone-driven horizontal cells in the rabbit retina. *J Neurophysiol* 57:645–659.
- Massey SC, Miller RF. 1990. N-methyl-D-aspartate receptors of ganglion cells in the rabbit retina. *J Neurophysiol* 63:16–30.
- Matute C, Streit P. 1986. Monoclonal antibodies demonstrating GABA-like immunoreactivity. *Histochemistry* 86:147–157.
- Morigawa K, Vardi N, Sterling P. 1995. Immunostaining for glutamate receptor subunits in mammalian retina. *Soc Neurosci Abstr* 21[part2]:901.
- Morrissey J, McCracken R, Ishidoya S, Klahr S. 1995. Partial cloning and characterization of an arginine decarboxylase in the kidney. *Kidney Intl* 47:1458–1461.
- Mosbacher J, Schoepfer R, Moyner H, Burnashev N, Seeburg P, Ruppersburg JP. 1994. A molecular determinant for submillisecond desensitization in glutamate receptors. *Science* 266:1059–1062.
- Müller F, Greferath U, Wässle H, Wisden W, Seeburg P. 1992. Glutamate receptor expression in the rat retina. *Neurosci Lett* 138:179–182.
- Nakajima Y, Iwakabe H, Akazawa C, Nawa H, Shigemoto R, Mizuno N, Nakanishi S. 1993. Molecular characterization of a novel retinal metabotropic glutamate receptor mGluR6 with a high agonist selectivity for L-2-amino-4-phosphonobutrate. *J Biol Chem* 268:11868–11873.
- Nakatani K, Yau K-Y. 1988. Calcium and magnesium fluxes across the plasma membrane of the toad rod outer segment. *J Physiol* 395:695–725.
- Partin KM, Fleck MW, Mayer ML. 1996. AMPA receptor flip/flop mutants affecting deactivation, desensitization, and modulation by cyclothiazide, aniracetam and thiocyanate. *J Neurosci* 16:6634–6647.
- Paternain AV, Morales M, Lerma J. 1995. Selective antagonism of AMPA receptors unmasks kainate receptor-mediated responses in hippocampal neurons. *Neuron* 14:185–189.
- Peng Y-W, Blackstone CD, Haganir RL, Yau KW. 1995. Distribution of glutamate receptor subtypes in the vertebrate retina. *Neuroscience* 66:483–497.
- Picco C, Menini A. 1993. The permeability of the cGMP-activated channel to organic cations in retinal rods of the tiger salamander. *J Physiol* 460:741–758.
- Piletz JE, Chikkala DN, Ernsberger P. 1995. Comparison of the properties of agmatine and endogenous clonidine-displacing substance at imidazoline and alpha-2 adrenergic receptors. *J Pharmacol Exp Ther* 272:581–587.
- Puro DG. 1991. Stretch-activated channels in human retinal Müller cells. *Glia* 4:456–460.
- Puro DG, Yuan JP, Sucher NJ. 1996. Activation of NMDA receptor-channels in human retinal Müller glial cells inhibits inward-rectifying potassium current. *Visual Neurosci* 13:319–326.
- Qin P, Pourcho RG. 1996. Distribution of AMPA-selective glutamate receptor subunits in cat retina. *Brain Res* 710:303–307.
- Qwik M. 1985. Inhibition of nicotinic receptor mediated ion fluxes in rat sympathetic ganglia by bungarotoxin fraction II-S1: a potent phospholipase. *Brain Res* 325:79–88.
- Raasch W, Regunathan S, Li G, Reis DJ. 1995. Agmatine, the bacterial amine, is widely distributed in mammalian tissues. *Life Sci* 56:2319–2330.
- Rang HP, Ritchie JM. 1988. Depolarization of nonmyelinated fibers of the rat vagus nerve produced by activation of protein kinase C. *J Neurosci* 8:2606–2617.
- Regunathan S, Feinstein DL, Raasch W, Reis DJ. 1995. Agmatine (decarboxylated arginine) is synthesized and stored in astrocytes. *Neuroreport* 6:1897–1900.
- Reith MEA. 1990. Characteristics of [14C] guanidinium accumulation in NG 108–15 cells exposed to serotonin 5-HT<sub>3</sub> receptor ligands and substance P. *Eur J Pharmacol* 188:33–41.
- Robinson SR, Hampson ECGM, Munro MN, Vaney DI. 1993. Unidirectional coupling of gap junctions between neuroglia. *Science* 262:1072–1074.
- Roche KW, Haganir RL. 1995. Synaptic expression of the high-affinity kainate receptor subunit KA2 in hippocampal cultures. *Neuroscience* 69:383–393.
- Sasaki T, Kaneko A. 1996. L-glutamate-induced responses in OFF-type bipolar cells of the cat retina. *Vision Res* 36:787–795.
- Sekiguchi M, Fleck MW, Mayer ML, Takeo J, Chiba Y, Yamashita S, Wada K. 1997. A novel allosteric potentiator of AMPA receptors: 4-[2-(phenylsulfonylamino)ethylthio]-2,6-difluoro-phenoxyacetamide. *J Neurosci* 17:5760–5771.
- Shank RP, Schneider CR, Tighe JJ. 1987. Ion dependence of neurotransmitter uptake: inhibitory effects of ion substitutes. *J Neurochem* 49:381–388.
- Slaughter MM, Miller RF. 1981. 2-Amino-4-phosphonobutyric acid: a new pharmacological tool for retina research. *Science* 211:182–185.
- Slaughter MM, Miller RF. 1983a. Bipolar cells in the mudpuppy retina use an excitatory amino acid neurotransmitter. *Nature* 303:537–538.
- Slaughter MM, Miller RF. 1983b. An excitatory amino acid antagonist blocks cone input to sign-conserving second-order retinal neurons. *Science* 219:1230–1232.
- Stell WK, Lightfoot DO. 1975. Color-specific interconnections of cones and horizontal cells in the retina of the goldfish. *J Comp Neurol* 159:473–502.
- Sun MK, Regunathan S, Reis DJ. 1995. Cardiovascular effects of agmatine, a “clonidine-displacing substance,” in conscious rabbits. *J Clin Exp Hypertension* 17:115–128.
- Uchihori Y, Puro DG. 1993. Glutamate as a neuron-to-glia signal for mitogenesis: role of glial N-methyl-D-aspartate receptors. *Brain Res* 613:212–230.
- Vaney D. 1990. The mosaic of amacrine cells in the mammalian retina. *Progr Retinal Res* 9:49–100.
- Velte TJ, Yu W, Miller RF. 1997. Estimating the contributions of NMDA and non-NMDA currents to EPSPs in retinal ganglion cells. *Visual Neurosci* 14:999–1014.
- Washburn MS, Numberger M, Zhang S, Dingledine R. 1997. Differential dependence on GluR2 expression of three characteristic features of AMPA receptors. *J Neurosci* 17:9393–9406.
- Wässle H, Grünert U, Martin PR, Boycott BB. 1994. Immunocytochemical characterization and spatial distribution of midrange bipolar cells in the macaque monkey retina. *Vision Res* 34:561–579.
- Wenzel A, Benke D, Mohler H, Fritschy J-M. 1997. N-methyl-D-aspartate receptors containing the NR2D subunit in the retina are selectively expressed in rod bipolar cells. *Neuroscience* 78:1105–1112.
- Wright EM, Loo DDF, Turk E, Hirayama B. 1996. Sodium cotransporters. *Curr Opin Cell Biol* 8:468–473.
- Yamashita M, Wässle H. 1991. Responses of rod bipolar cells isolated from the rat retina to the glutamate agonist 2-amino-4-phosphonobutyric acid (APB). *J Neurosci* 11:2372–2382.
- Yazajian B, Fain GL. 1992. Excitatory amino acid receptors on isolated retinal ganglion cells from the goldfish. *J Neurophysiol* 67:94–107.
- Yoshikami D. 1981. Transmitter sensitivity of neurons assayed by autoradiography. *Science* 212:929–930.
- Zhou ZJ, Fain GL. 1995. Neurotransmitter receptors of starburst amacrine cells in rabbit retinal slices. *J Neurosci* 15:5334–5345.
- Zhou ZJ, Fain GL, Dowling JE. 1993. The excitatory and inhibitory amino acid receptors on horizontal cells isolated from the white perch retina. *J Neurophysiol* 70:8–19.
- Zhou ZJ, Marshak DM, Fain GL. 1994. Amino acid receptors of midrange and parasol ganglion cells in primate retina. *Proc Natl Acad Sci USA* 91:4907–4911.